

Article

# Six ‘Must-Have’ Minerals for Life’s Emergence: Olivine, Pyrrhotite, Bridgmanite, Serpentine, Fougérite and Mackinawite

Michael J. Russell <sup>1,\*</sup> and Adrian Ponce <sup>2</sup> 

<sup>1</sup> Dipartimento di Chimica, Università degli Studi di Torino, via P. Giuria 7, 10125 Turin, Italy

<sup>2</sup> Jet Propulsion Laboratory, California Institute of Technology, Pasadena, CA 91109, USA; adrian.ponce@jpl.nasa.gov

\* Correspondence: michaeljohn.russell@unito.it or Michaeljrussell80@gmail.com; Tel.: +39-351-8247070

Received: 19 October 2020; Accepted: 14 November 2020; Published: 19 November 2020



**Abstract:** Life cannot emerge on a planet or moon without the appropriate electrochemical disequilibria and the minerals that mediate energy-dissipative processes. Here, it is argued that four minerals, olivine ( $[\text{Mg}>\text{Fe}]_2\text{SiO}_4$ ), bridgmanite ( $[\text{Mg},\text{Fe}]\text{SiO}_3$ ), serpentine ( $[\text{Mg},\text{Fe}]_{2-3}\text{Si}_2\text{O}_5[\text{OH}]_4$ ), and pyrrhotite ( $\text{Fe}_{(1-x)}\text{S}$ ), are an essential requirement in planetary bodies to produce such disequilibria and, thereby, life. Yet only two minerals, fougérite ( $[\text{Fe}^{2+}_6\text{Fe}^{3+}_{6(x-1)}\text{O}_{12}\text{H}_2(7-3x)]^{2+} \cdot [(\text{CO}_3^{2-}) \cdot 3\text{H}_2\text{O}]^{2-}$ ) and mackinawite ( $\text{Fe}[\text{Ni}]\text{S}$ ), are vital—comprising precipitate membranes—as initial “free energy” conductors and converters of such disequilibria, i.e., as the initiators of a  $\text{CO}_2$ -reducing metabolism. The fact that wet and rocky bodies in the solar system much smaller than Earth or Venus do not reach the internal pressure ( $\geq 23$  GPa) requirements in their mantles sufficient for producing bridgmanite and, therefore, are too reduced to stabilize and emit  $\text{CO}_2$ —the staple of life—may explain the apparent absence or negligible concentrations of that gas on these bodies, and thereby serves as a constraint in the search for extraterrestrial life. The astrobiological challenge then is to search for worlds that (i) are large enough to generate internal pressures such as to produce bridgmanite or (ii) boast electron acceptors, including imported  $\text{CO}_2$ , from extraterrestrial sources in their hydrospheres.

**Keywords:** astrobiology; Hadean; carbonic ocean; proton gradient; redox gradient; solar system; submarine alkaline vents; emergence of life; exoplanets

---

... molecular physics is the true basis of biology. [1]

... physics approximates biology because there is no such thing as an organism at thermodynamic equilibrium. [2]

## 1. Introduction

Life being an emergent far-from-equilibrium, actively dynamic structure suggests that astrobiological exploration should focus on wet worlds where mantle convection, coupled to hydrothermal convection, resulted in strong electrochemical disequilibria commensurate with life and its emergence [3–10]. It is not enough to base astrobiological exploration on the detection of wafts of organic molecules that, after all, merely hint at the presence of reduced carbon. Indeed, most planets and moons in our outer solar system were accreted from native iron meteorites and carbonaceous chondrites (CCs), and consequently likely amassed hydrocarbon fuel aplenty as observed on Titan and possibly Enceladus [11–13]. What often seems to be missing is the other pole for the ‘battery’—the oxidants or electron acceptors [14].

A fundamental understanding of what drove life into being on our planet requires knowledge of how inorganic minerals, accreted from the solar disc, responded to physicochemical pressure and

stresses induced by convection and differentiation in an early magma ocean [7,8,15,16]. These dynamic processes provided the ‘bio-elements’ C, H, O, N, P, S, the transition metal sulfide and oxide clusters and both the reductants and oxidants necessary for life’s emergence [17–22]. Since the primordial hydrogen atmosphere was blown beyond the snow line by the intense solar wind [23], volatiles degassing from the mantle would have included carbon dioxide, nitrogen and water [24,25]. Minor concentrations of oxidants such as nitrogen oxides (NO<sub>x</sub>) were generated from these gases, mainly through the action of cloud-to-cloud-lightning in the atmosphere and occasional coronal mass injections reaching several GeV—the NO<sub>x</sub> thenceforth to be rained into the early ocean [26–29].

One fuel necessary for life’s emergence on Earth was H<sub>2</sub>—or the electrons prized therefrom—degassing from heterogeneous sources deep in the mantle and at the core-mantle boundary [30–33]. This hydrogen would have been joined by formate and methane, reduced from CO<sub>2</sub> abiotically in the ~40 to 80 km thick Hadean ocean crust [34–39]. Apart from the ‘electricity’ provided by the oxidation of hydrogen, another driving force that couples with redox is the ‘proticity’ provided by a proton gradient [3,40]. Together, these are the reductants and oxidants and gradients responsible for life’s emergence as detailed in the submarine alkaline vent theory (AVT) (Figures 1 and 2) [4,41–43]—a theory receiving a recent endorsement from the microfluidic experiments of Hudson and his collaborators involving nickel in an Fe(Ni)S barrier as catalyst as well as a steep proton gradient [44].

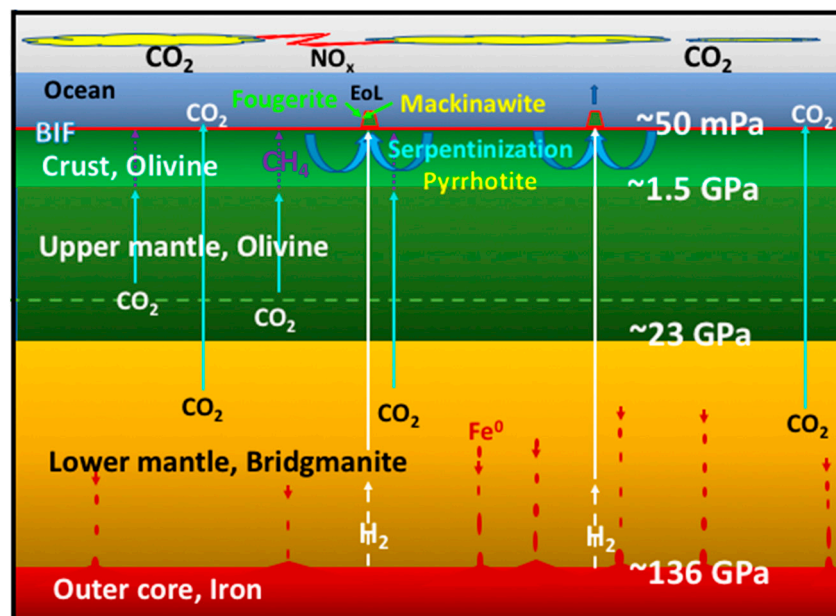


**Figure 1.** Cross-section sketch of Earth in the Hadean showing the mechanisms—the coupled engines—that promote the conditions for the emergence of life (EoL). The result is the generation of precipitate hydrothermal mounds comprising fougérite, subordinate mackinawite and silica gel (Figure 2) [39,45–47]. The diagram indicates the whereabouts of the six ‘must-have’ mineral phases discussed in the text. Pressure in excess of 23 GPa metamorphoses olivine and ringwoodite to the perovskite mineral, bridgmanite, leading to the disproportionation of ferrous iron to Fe<sup>0</sup> and Fe<sup>3+</sup> in the early magma ocean. The gravitation of the native iron toward the core left a mantle enriched in ferric iron buffered at quartz-fayalite-magnetite (QFM: SiO<sub>2</sub>-Fe<sup>2+</sup><sub>2</sub>SiO<sub>4</sub>-Fe<sup>2+</sup>Fe<sup>3+</sup><sub>2</sub>O<sub>4</sub>) [15,48]. CO<sub>2</sub>, degassing rapidly from olivine-bearing komatiitic lavas and intrusives fed from super-plumes from deep within the relatively oxidized hot mantle, bubbles up at high pressure onto the ocean floor, producing a carbonic ocean with extreme pH in relatively quiescent periods of between 5 and 5.5 units [35,49–53]. Cloud-to-cloud lightning produces NO<sub>x</sub> that, when dissolved in the ocean, generates nitrate and nitrite ions [28]. Any CO<sub>2</sub> trapped in the thick Hadean oceanic crust slowly converts to CH<sub>4</sub> and formate below ~400 °C, some of which is entrained in the moderate temperature alkaline hydrothermal systems [37,39,46,54–56]. The partial dissolution of pyrrhotite and the hydration and oxidation of olivine to serpentine in the oceanic crust through convective circulation of ocean water

generates the moderate temperature alkaline springs bearing  $\text{HS}^-$  [39,46]. These alkaline fluids also entrain  $\text{H}_2$  emanating from the mantle and core-mantle boundary [37,39]. Up to 80 mmol/liter of ferrous iron and subordinate transition metals derived from a myriad of  $\leq 410^\circ\text{C}$  acidic springs (not shown) were pumped into the early acidulous Hadean ocean where much of the iron remained in supersaturated solution [45,57,58]. For the most part this iron was only precipitated as fougérite and subordinate mackinawite (accompanied by silica gel) on meeting submarine alkaline hydrothermal springs bearing  $\leq 10$  micromoles of the bisulfide ( $\text{HS}^-$ ) and 0.1 to 10 millimoles of the hydroxyl ion ( $\text{OH}^-$ ). The result was the generation of precipitate hydrothermal mounds comprising fougérite, subordinate mackinawite and silica gel [39,45–47]. Peripheral fougérite also gave rise to the Banded Iron Formations (BIF) [59,60]. In alkaline vent theory (AVT) one of the fougérite-mackinawite-silica mounds so precipitated on the ocean floor was the hatchery of life (EoL: Emergence of Life) [4,39,41,43,61].

In order to produce these fuels, redox and pH gradients that mediated life's emergence required just six 'must-have' minerals (Figure 1) [42,62]. Our study brings to the fore the centrality of physical and mechanical (i.e., conformational) responses of some of these minerals as disequilibrium-converting engines, or as components thereof [2,9,14,18,37,63–67]. For, as we learnt from the long history of continental drift debate, any theory devoid of mechanisms, i.e., engines, is doomed to a short life-span [18,62,68]. These six minerals are divided into two groups:

1. The first group contains the four minerals setting the stage for the geochemical disequilibria that drives life into being through the macro-engines of convection, to give rise to a  $\text{CO}_2$ -rich, transition-metal bearing acidulous Hadean ocean [39,46].
2. The second group contains the two mineral precipitates—ferrous iron-rich oxyhydroxides and monosulfides—constituting a membrane that keeps the two contrasting fluids from immediate mixing. In AVT the oxyhydroxides are the disequilibria-converting nano-engines and solid electrolytes, while the monosulfides are the electron conductors and proto-hydrogenases. Combined, they have the potential to mediate the disequilibria and bring life into being (Figure 2) [9].

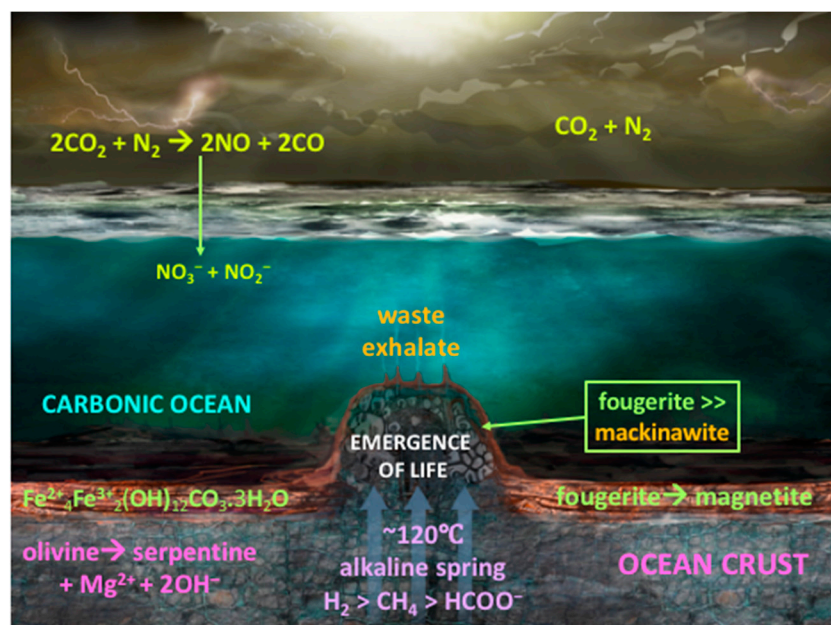


**Figure 2.** The Hadean Earth as a water world [41]. The ocean was carbonic and nitrate/nitrite-bearing, with pH in relatively quiescent periods between 5 and 5.5, having been injected from below with high pressure  $\text{CO}_2$  exhalations from the mantle; from solidifying komatiitic lavas and intrusive magmas in equilibrium with QFM, and from above with  $\text{NO}_x$  produced by cloud-to-cloud lightning [15,28,51,53]. The partial dissolution of pyrrhotite and the hydration and oxidation of olivine to serpentine in the ~40–80 km thick Hadean oceanic crust generates the moderate temperature alkaline springs bearing  $\text{HS}^-$

as well as CH<sub>4</sub> and formate produced in the crust by the reduction (hydrogenation) of CO<sub>2</sub> [35,37,39,46,54,55]. It also entrains H<sub>2</sub> emanating from the mantle and core-mantle boundary [31,32,69]. Transition metals derived from myriad ≤410 °C acidic springs (not shown) [45,57,58] and present in metastable state in the ocean, are spontaneously precipitated as fougérite and subordinate mackinawite on meeting the alkaline hot springs to produce the hydrothermal mound argued to be the hatchery of life as in Figure 1 (EoL) [4,39,41,43,61].

## 2. Four Minerals to Set the Stage for Life's Emergence

The four essential minerals in planetary bodies needed to produce the chemical disequilibria and materials required for life's emergence are olivine ([Mg>Fe]<sub>2</sub>SiO<sub>4</sub>), bridgmanite ([Mg,Fe]SiO<sub>3</sub>), serpentine ([Mg,Fe]<sub>2-3</sub>Si<sub>2</sub>O<sub>5</sub>[OH]<sub>4</sub>) and pyrrhotite (Fe<sub>(1-x)</sub>S). We begin with olivine, a ubiquitous mineral contributing to the primary extrusive and intrusive basaltic or komatiitic ocean floor, crust and upper mantle (originally as short-lived magma oceans [70]) to a myriad of putative planets—the precursor to suites of minerals produced through the stressors of pressure, thermal gradients and hydration. We proceed with the most abundant of these—bridgmanite (Mg,Fe)SiO<sub>3</sub>—which is hidden at depth out of reach of spectroscopy. Its occurrence must be gauged experimentally from a planet's metamorphic response to size and dehydration and as supported by seismic profiles [15,71]. Hydration of olivine makes for the alkaline nature of the feeders to life in the AVT, while pyrrhotite is the dominant abiogenic source of the sulfur [39,44,46]. Olivine and pyrrhotite react with hydrothermal solutions at ≤150 °C to produce the serpentine mineral and the alkaline fluids bearing ≤10 millimoles of hydroxyl and ≤10 micromoles of bisulfide [39,56,72]. The result is a strong pH disequilibrium between the alkaline fluid (pH ~11 to 11.5) and the relatively low, though varying, pH of the early ocean (~pH 5 to 5.5) [43,49,50,53,73]. The presence of bridgmanite, as inferred from experiments, indicates a mantle in equilibrium with carbonate or carbon dioxide, the feedstock of life, but in disequilibria with hydrogen emanating from core, mantle and crust [31,32,69].

### 2.1. Olivine (Mg>Fe)<sub>2</sub>SiO<sub>4</sub>

This olive colored magnesium ferrous-iron silicate comprises much of the modern mafic and ultramafic upper mantle down to ~410 km, the basaltic ocean floor to our planet, numerous volcanic islands (e.g., the Galapagos), and in upthrust (obducted) elements of ocean floor in mountain belts, the so-called ophiolites (e.g., Cyprus). Olivine also contains significant traces of water, nickel, manganese and, on occasion, pyrophosphate [74–77]. Both the nickel and manganese may be released to acidic hydrothermal solutions, while the pyrophosphate may have been released through high temperature acidic degassing [78]. However, mantle olivines appear to have low phosphate contents (typically 10 to ~60 ppm P, but reaching 0.2% on occasion) [79,80]. On land, soils developed over olivine-bearing basaltic rocks have been sought throughout the ages for their fertility [81,82]. And today basalts are even quarried and crushed as a general-purpose fertilizer and as a mitigating agent of anthropogenic CO<sub>2</sub> increase [10,83].

In the Hadean (4.5 to 4.0 billion years before present (Ga)), in what is now the Earth's mantle, olivine began to precipitate in a relatively short-lived magma ocean and in super plumes induced through giant impacts [8,70,84,85]. A depth of 410 km marks the beginning of a transition zone in the mantle. Under these pressures, the orthorhombic olivine crystals, with a density (ρ<sub>0</sub>) of ~3.3 g/cm<sup>3</sup>, give way to the compositionally equivalent, though denser spinel-structured ringwoodite (ρ<sub>0</sub> = 3.65 g/cm<sup>3</sup>) [86,87], with the likely expulsion of trapped water at high pore pressure [88–90]. This pressure-induced mineral transition to ringwoodite is only a prelude to the much more significant 'collapse' of that spinel structure to a silicate perovskite crystal type with a density of ~4.2 g/cm<sup>3</sup> [91]. The perovskite that comprises the lower mantle is designated 'bridgmanite', our next concern. This transition produces the sharp upper-to-lower mantle discontinuity at a depth of 660 km, broken on occasion by those giant impact-induced buoyant super plumes [15,84,90,92–95] (Figure 3).

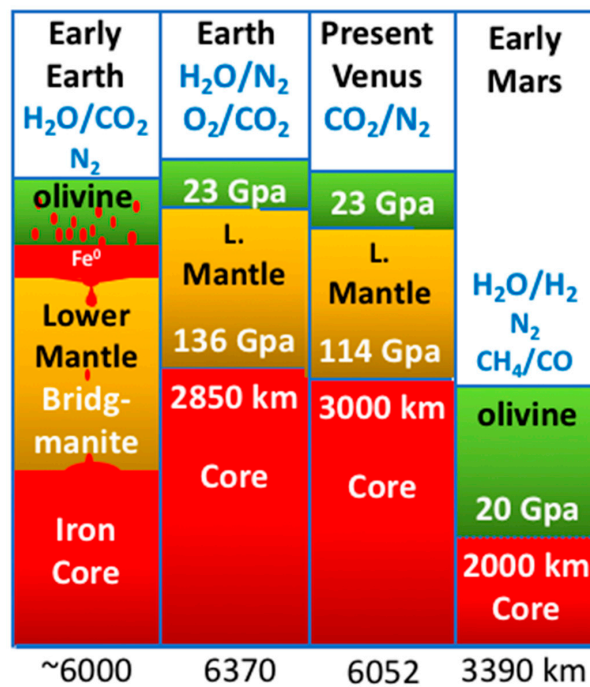


**Figure 3.** Depth and pressure comparisons between the early Earth (with native iron gravitating to the core), and present-day Earth, Venus and Mars. Bridgmanite is produced at pressures of ~21–23 Gpa and marks the upper to lower mantle (ringwoodite to bridgmanite) transition zone on Earth and Venus, a pressure barely reached on Mars. It follows that present-day Earth has a mantle at QFM, as does Venus. Impact-induced mantle super plumes were also responsible for the partial homogenization of the mantles of Earth and probably Venus [84,96]. The Martian mantle is likely to be far more reduced, hydrogen-buffered around iron-wüstite (Fe:FeO) [97]. Assuming magma oceans occupied portions of all three planets, it follows that the atmospheres of the early Earth and probably early Venus comprised CO<sub>2</sub> and H<sub>2</sub>O, whereas the early atmosphere/hydrosphere of Mars consisted of H<sub>2</sub> + H<sub>2</sub>O > CH<sub>4</sub> + CO. A percentage of N<sub>2</sub> is common to all [98]. Figure based on [5,16,20,99–101].

## 2.2. Bridgmanite (Mg,Fe)SiO<sub>3</sub>

Bridgmanite, the silicate perovskite, is the most abundant mineral in the Earth, comprising ~80% of the lower mantle, with the remainder being made up of magnesiowüstite ([Mg,Fe]O) and Ca-perovskite (~Ca[Fe,Ti]O<sub>3</sub>) [92]. The lower mantle extends from the 660 km (23 GPa) discontinuity down to the outer core boundary at 2900 km (135 GPa) (Figures 1 and 3) [57,95,102]. Yet its presence was only initially surmised from experimental work [93]. This is because bridgmanite is a very rare mineral, generally found only in meteorites where it is generated by transitory high shock waves pressures of 18 to 25 GPa [95,103–105].

So why is bridgmanite so central to astrobiology? The short answer is that its formation generates a mantle with an oxygen fugacity (i.e., an effective partial pressure) high enough to render much of the carbon into its most oxidized form, i.e., as carbon dioxide, the main substrate of life [1,54,106]. This CO<sub>2</sub>-producing chemistry is facilitated by the ‘collapse’ of the ringwoodite lattice structure to the relatively condensed perovskite lattice. Perovskite needs a metal ion with a valency of three to build its structure. This ion is generally Al<sup>3+</sup>, but there is an inadequate supply of aluminum in the upper mantle to satisfy this requirement, and none at all in ringwoodite that occupies a lower pressure zone just above the 660 km discontinuity. The need for a trivalent metal ion is satisfied by the forced disproportionation of the Fe<sup>2+</sup> ions in the olivine/ringwoodite lattices to Fe<sup>3+</sup> and Fe<sup>0</sup> (metallic iron) [15,57,107]. While the Fe<sup>3+</sup> fulfilled this need in the perovskite structure of bridgmanite, the newly orphaned high density Fe<sup>0</sup> would have been excluded to the surrounds and much of it sunk to the core as the magma ocean cooled, leaving the mantle oxidized enough to be buffered

by quartz-fayalite-magnetite (QFM). With iron being partly oxidized in magnetite ( $\text{Fe}^{2+}\text{Fe}_2^{3+}\text{O}_4$ ), at mantle temperatures much of the carbon was forced into the 4+ oxidation state, i.e., as  $\text{CO}_2$  (Figures 1 and 2) [5,48,55,92,100,108–111]. This carbon dioxide-producing physical chemistry facilitated by the perovskites produced an  $\text{H}_2\text{O}$ - and  $\text{CO}_2$ -dominated atmosphere that dates from the final stages of Earth's accretion [15,112].

This theory whereby the surviving magnetite controls the effective partial pressure of  $\text{CO}_2$  has been put to various tests and investigations, notably by a demonstration that accounts for the 'heavy' iron isotope composition of the Earth's basalts as compared to similar samples from Mars and the asteroid Vesta [113]. In fact, Martian basalts are generally much more reduced than those of Earth [114,115]. Indeed, judging from Martian meteorites, it appears that the redox state of the Martian mantle is buffered around, or even below, the iron-iron oxide (iron-wüstite,  $\text{Fe}:\text{FeO}$ ) boundary [97]. And it is calculated that the core/mantle boundary in Mars is defined by ringwoodite ( $\text{Mg,Fe}$ ) $_2\text{SiO}_4$  to solid iron [116–118]. In such a case gases evolved from the reduced Martian magmas and resulting from giant impacts would have mainly comprised hydrogen, water vapour, methane and carbon monoxide [8,16]. In fact, notwithstanding earlier arguments [119], as the olivine/ringwoodite-to-bridgmanite transition is not realized (which requires a pressure of 23 GPa to trigger the said transition), planets the size of Mars or smaller are much less likely to emit large quantities of  $\text{CO}_2$ —the staple of life—through degassing and vulcanism [16,20,48,116].

### 2.3. Pyrrhotite $\text{Fe}_{(1-x)}\text{S}$ ( $x = 0$ to $0.2$ )

Accompanying the olivine in the mantle was the partially oxidized (sulfidized) iron sulfide pyrrhotite, along with its nickel-bearing equivalent pentlandite ( $[\text{Fe,Ni}]_9\text{S}_8$ ) [120]. It also occurs within, or more generally at the base of komatiitic lava flows, introduced as a sulfide melt along with the silicate lavas [121]. The mineral is vital as the source of sulfur dissolving in hydrothermal solutions as a required constituent of bioorganic molecules. During alkaline hydrothermal convection, some of the sulfur component of the pyrrhotite is released to solution as bisulfide ( $\text{HS}^-$ ), to be precipitated, on meeting with ferrous iron from the ocean as a minor  $\text{FeS}$  (mackinawite) component of the alkaline hydrothermal mound (Figures 1 and 2) [3,39,46,122–125].

### 2.4. Serpentine $(\text{Mg,Fe})_{2-3}\text{Si}_2\text{O}_5(\text{OH})_4$

If olivine is subjected to interaction with water at temperatures up to  $\sim 300$  °C it hydrates exothermically in a process called serpentinization, the main thermal drive to the alkaline convective hydrothermal cells [126]. As the serpentine has a greater volume and lower density than olivine the effect is to force fine-scale cracking of the upper crust [127]. In the AVT the mechanism of serpentinization was invoked to predict the occurrence of submarine open system hydrothermal convection cells that would generate off-ridge alkaline springs [3,55,128]. These springs would feed the reducing agent hydrogen in the spring waters as a source of electrons to generate organic molecules in the resulting hydrothermal precipitate mound (Figures 1 and 2) [4,52]. In this scenario the serpentinizing system is an 'upstream' mechanism or engine whose output feeds the hatchery of life in a submarine alkaline spring mound as electrons, methane and formate interact in the mineral membrane with carbon dioxide and nitrate and nitrite (Figure 2) [4,14,62,129,130].

However, Tutolo et al. [131] show that in the silica-rich Hadean ocean, minimal hydrogen would be generated at nearly two orders of magnitude lower than we had formerly assumed. Nevertheless, we do know that large quantities of hydrogen would have degassed from sources in the Earth's mantle and from the mantle/core boundary [31,32,103,132–134]. Also, Tutolo et al. [131] did demonstrate that the pH contrast at the Hadean submarine alkaline—as an ambient proton motive force—to be up to two orders of magnitude greater than we had first surmised [4]. This is significant because Hudson and his collaborators [44] have shown that in a test of a version of AVT, the formic acid ( $\text{HCOOH}$ ) produced from  $\text{CO}_2$  derives its hydrogen from external protons in the presence of hydrogen at 1.5 bars [44].

One geophysical difference between early Earth and now, is the likelihood that whereas the mantle was substantially hotter in the Hadean [34,135], the oceanic crust was stagnant prior to the onset of plate tectonics produced by volcanic over-, inter- and under-plating, fed from super plumes. Hence, at certain locations, the thermal gradient in dormant sections would have been much lower on early Earth [35,37]. At the same time radial and concentric fracturing produced by mantle bulges over and around super plume heads likely penetrated through the 40 to 80 km thickness of the crust. Moreover, “downward-excavating” open hydrothermal convective serpentinizing systems may have plumbed substantially deeper than they do today, leaching more methane [136,137], and lasting even longer than the  $\sim 10^5$  years estimated by Ludwig et al. [138]. As  $\text{CO}_2$  escaped from the mantle, it would be reduced to  $\text{CH}_4$  along the fracture walls at temperatures below  $\sim 400$  °C, before the methane was entrained in the aforementioned hydrothermal cells [37,54,55,136]. This methane is another potential fuel, one that could have introduced abiotically reduced carbon to a putative metabolism [39,55,130,139–142] (Figures 1 and 2).

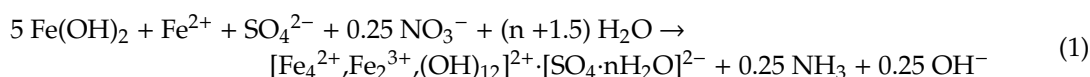
We conclude that the disequilibria at the alkaline spring/acidulous ocean interface was theoretically sufficient to drive and nurture emergent life [38,39,129,130,142–144].

### 3. Two Minerals to Make Life Happen

In the presence of the disequilibria produced by the four minerals that set the stage for life’s emergence, two minerals, fougurite ( $[\text{Fe}^{2+}_6\text{Fe}^{3+}_{6(x-1)}\text{O}_{12}\text{H}_{2(7-3x)}]^{2+} \cdot [(\text{CO}_3^{2-})_3\text{H}_2\text{O}]^{2-}$ ) and mackinawite ( $\text{Fe}[\text{Ni}]\text{S}$ ), are vital as initial “free energy” conductors and converters of such disequilibria, and are considered as the initiators of a  $\text{CO}_2$ -reducing metabolism in a membrane constituted of these same minerals [43]. The iron-bearing oxyhydroxides and subordinate sulfide are precipitated at the ocean-crust interface where the alkaline hydrothermal fluids meet the acidulous ocean water bearing iron and other transition elements fed to the ocean from the  $\leq 410$  °C acidic springs [45,57,58]. But because the molarity of hydroxide in the alkaline fluids is so much higher than that of the sulfide, the oxyhydroxide fougurite (green rust) dominates the precipitates [56] (Figure 4) rather than iron sulfide as previously thought [4,43,145].

#### 3.1. Fougurite $[\text{Fe}^{2+}_6\text{Fe}^{3+}_{6(x-1)}\text{O}_{12}\text{H}_{2(7-3x)}]^{2+} \cdot [(\text{CO}_3^{2-})_3\text{H}_2\text{O}]^{2-}$

The green rust mineral fougurite is a mixed-valence redox-flexible semi-conducting naturally-occurring anionic clay, doped with  $\text{Mg}^{2+}$ ,  $\text{Ni}^{2+}$ ,  $\text{Mn}^{2+}$ , and  $\text{Co}^{2+}$  [146,147]. Fougurite’s extensive inner surfaces appear to provide the ‘mechanistic’ potential to fill the roles of the redox- and pH-converter that enabled life’s emergence by driving endergonic—thermodynamically uphill—processes [41,43,62,130,145,148–151]. And there was certainly no want for fougurite in the all-enveloping early ocean—the mineral precursor to the diagenetic magnetite comprising the first known banded iron formation outcropping in western Greenland [45,59,60,152–154]. Mimicking this natural process of precipitation and transformation, Konstantinos Simeonidis and his collaborators [155] have generated green rust on a path to nanometric idiomorphic crystals of magnetite—a mineral with potential in catalysis, biotechnology and water remediation, though it is inimical to membrane formation. Their continuous processing mechanism employed nitrate ions to oxidize ferrous iron in aqueous solution as demonstrated by Hansen and collaborators [156] and adopted by Russell and colleagues [41,43] in the AVT (eqn 1 from Asimakidou et al., [155]):



Following from demonstrations of the variable valence fougurite to act as an inorganic nitrate/nitrite reductase, Barge and her collaborators show that ammonium can aminate pyruvate (itself theoretically provided by hydrogenation of  $\text{CO}_2$  on the mineral greigite) [157] to the amino acid alanine in the presence of fougurite [157,158] (Figures 4 and 5). Moreover, Tosca and collaborators [73] demonstrate

the generation of hydrogen as green rust is oxidized by water which would provide another source of  $H_2$  at an alkaline vent. And Arrabito and collaborators [159] demonstrate a general consanguinity between life and green rust as they also draw attention to how the biocompatibility of the double layer hydroxides, including green rust, have been extensively exploited in the biomedical industry. Yet to be tested are (i) the presumed potential of green rust situated in the membrane to also act as a proton wire, a proton pyrophosphatase, methane monooxygenase, polymerase and (ii) as an engine of synthesis in the production of aromatic rings (cf. quinones and flavins) [62,65,130,145,150,151,160–162].

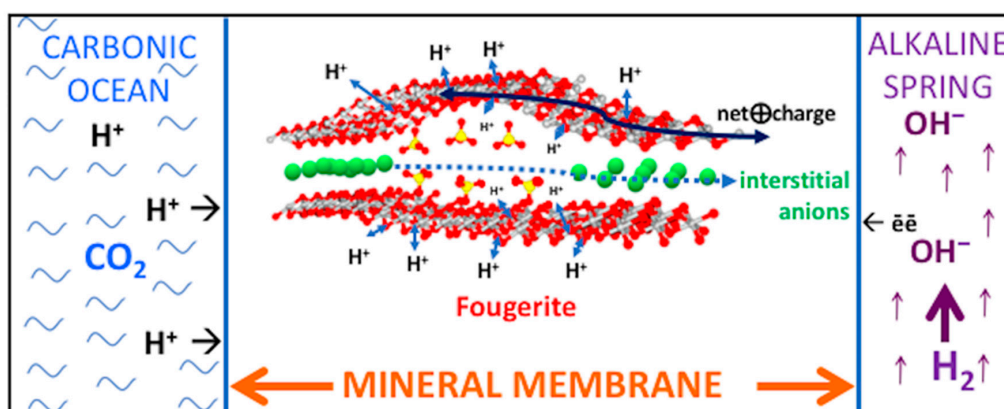


**Figure 4.** Cross-section of two individual iron oxyhydroxide layers of the double layered mineral fougerite. In the AVT fougerite nano- to micro-crystals comprise the mid and outer portions of an inorganic membrane (see Figure 5) precipitated by—but separating the acidulous ocean from—the alkaline hydrothermal spring waters [145,150,151]. The detailed structure shows the contrasting heights of the interstitial space (the interlayer) between two layers of a redox-flexible fougerite nanocrystal (e.g.,  $Fe^{2+}_4Fe^{3+}_2[OH]_{12} \cdot CO_3 \cdot 3H_2O \rightleftharpoons Fe^{2+}_2Fe^{3+}_4O_2[OH]_{10} \cdot CO_3 \cdot 3H_2O$ ) (Figure 5). Intercalated between these inner surfaces are spherical ions (e.g., chloride and/or carbonate) forcing a gallery height of 0.75 nm, and tetragonal ions (e.g., sulfate and/or condensed phosphate,  $P_2O_5$  as in olivine) which expand the height to ~1.1 nm [163]. Stresses associated with such conformational flexuring may be measured in piconewtons, comparable to those operating in the motor protein myosin [164–166]. Any motion of charge along the Fe-oxyhydroxide layers will be accompanied by modifications in the pK values of the OH groups such that more oxidized  $Fe^{3+}$  sites will tend to deprotonate their ambient hydroxy groups, thus releasing  $H^+$  into the interstices [167]. Drift of  $Fe^{3+}$  sites has the potential to pull interstitial anions along the galleries to produce condensations and other reactions in this low entropy environment. In this scenario the fougerite mineral acts as a pump or nanoengine. For example, as the electron current is drawn toward the oxidants, so the 3+ charge on the iron atoms would migrate in the opposite direction with the potential to drag carboxylic anions from the outer periphery inwards to react with ammonium formed in the same structure and, therefrom, synthesize amino acids [43,156,158]. Electrons will hop in directions counter to the drift of the  $Fe^{3+}$  sites, while the hydrous interlayers could act as a proton wire whereby transport is facilitated by the grotthuss mechanism [162]. Note that the model nanocryst is just one of a myriad comprising the mineral membrane (cf. Figure 5).

Computer simulations have provided insights that help in the planning of such experiments [159,168–170]. And the relatively recent development of operando techniques should allow demonstrations of, for example, coupling of steep redox/pH gradients along the metal and hydrous layers respectively including reductive recharge, to the driving of other endergonic reactions [171]. Moreover, there is some theoretical support for seeing the interior galleries of double layer hydroxides such as fougerite offering the beginnings of a guidance or information system. The first consideration in this respect is to enquire, and investigate, how fougerite might couple to a fluctuating or a varying environment beyond mere ‘static’ determinism [146,172–174]. The greater the asymmetric response or rates of response to reversals of the driving force the more impact this would have on evolution [172,175]. Reactions along such paths that lead, at each step, to a limited autonomy through the development of

improved information systems should also result in a fuel-saving economy [172]. We turn next to the single layered sulfide, mackinawite, as a necessary support mineral.

### 3.2. Mackinawite Fe(Ni)S

Mackinawite—an electron conductor [176]—is the subordinate sulfide analogue of fougurite, precipitating with it at the submarine alkaline spring, and comprising a small inner portion of the membranes dividing ocean from alkaline hydrothermal solution (Figure 5) [56,177]. Although, like fougurite it is a layered mineral, Bourdoiseau and coworkers [178] have shown, against earlier expectations, that it includes no layered hydrous intercalations. However, mackinawite does retain its structure during partial oxidation, though not by the insertion of anions, but rather through the loss of  $\text{Fe}^{2+}$  to solution to maintain charge parity [178–180].

Nevertheless, like fougurite, mackinawite diadochically absorbs  $\text{Ni}^{2+}$ ,  $\text{Mg}^{2+}$ ,  $\text{Mn}^{2+}$ , and  $\text{Co}^{2+}$  in the ferrous iron site [61,160,181–184]. Indeed, nickeliferous mackinawite also had a protometabolic role in AVT [3,61,185]. Demonstrating the first “crack” in the kinetic barrier to life, i.e., one that offered the ‘escape route’ to an autotrophic protometabolism, Hudson and his collaborators [44] demonstrated the role of an Fe(Ni)S precipitate in the effective hydrogenation of  $\text{CO}_2$  to formate through the application of a steep pH gradient—one of the predictions of the AVT [3,42,186] (Figure 5).

In the hydrothermal conditions at the vent, as with fougurite [73], mackinawite maybe oxidized/sulfidized to greigite with the release of hydrogen and/or its absorption as electrons and protons (cf. the ‘cubane’ active centers to the affine iron-sulfur enzymes) [61,187]. Whether the conformational oxidation to greigite can be reversed in this nanoworld scenario is an open question. If so the two conformations might support action as a disequilibria converter, a possibility that also invites further research [188]. Judging from density functional theory (DFT) calculations, greigite ( $\text{Fe}_3\text{S}_4$ ) too has a further potential protometabolic role, that of catalyzing the hydrogenation of  $\text{CO}_2$ —via the reduction of the carbonyl moiety of the intermediate glyoxylic acid ( $\text{CHO-COOH}$ )—to acetic and pyruvic acids [157,189].

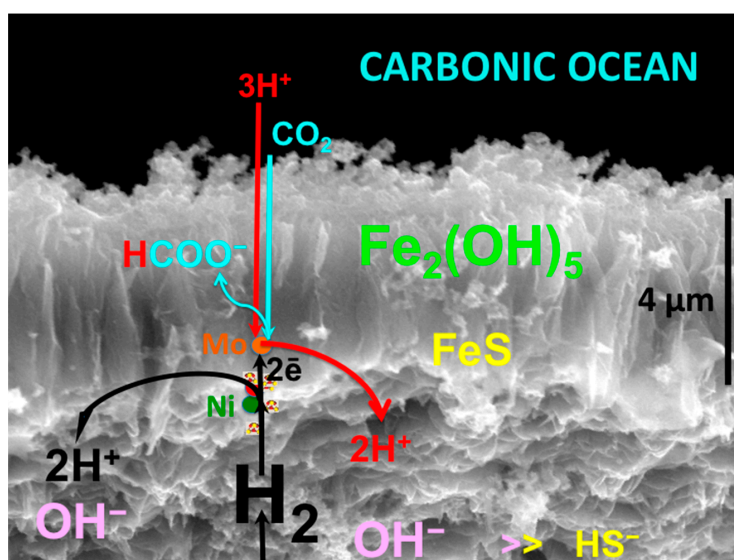


**Figure 5.** A putative reduction of  $\text{CO}_2$  in the Hadean ocean (top) to formate ( $\text{HCOO}^-$ ) in a membrane comprising the ‘must-have’ nickel-bearing minerals fougurite ( $\sim\text{Fe}_2[\text{OH}]_5$ ) (central and outer zone) and subordinate mackinawite ( $\text{FeS}$ ) (inner zone), dosed with molybdenum as further catalyst [56,190]. The alkaline hydrothermal solution occupies the bottom of the diagram. Formate generation is driven by protons from the ocean accessing the Ni-(and Mo-) dosed  $\text{FeS}$  nanocrystals through the outer fougurite layer [9,42,44,56,190,191]. In this speculative rendition, the formate is discharged into the hydrous interlayers of fougurite, a mineral known for mediating prebiotic biochemistry-like production (Table 1) [156,177]. To be compared to Hudson et al. [44] figures 1A, 3D and S28.

**Table 1.** The six ‘must-have’ Hadean minerals as they are thought to contribute to the emergence of life on Earth.

Mineral	Contribution and Consequence	References
Olivine	Upper mantle/crust: precursor to bridgmanite & serpentine	[74–77,79,80]
Bridgmanite	Lower mantle mineral produced by metamorphism of Fe <sup>2+</sup> /Mg-silicate so forcing disproportionation of the Fe <sup>2+</sup> as bridgmanite purloins Fe <sup>3+</sup> , effectively oxidizing the lower mantle as the orphaned Fe <sup>0</sup> gravitates to the core	[92,95,103,105,107]
Pyrrhotite	Source of bisulfide (HS <sup>−</sup> ) in the alkaline hydrothermal solutions	[3,39,46,120,121,123–125,192]
Serpentine	Hydration of olivine generates highly alkaline submarine springs with pH contrast with Hadean ocean of ~6 pH units	[3,4,38,39,55,126–131,136,137,142–144]
Fougerite	Dominant precipitate at vent, sufficiently complex as a membrane to have acted as embryonic life’s first disequilibria converter (as a general reductase, aminase, and possibly a polymerase and pyrophosphatase), H <sub>2</sub> generator and proton transfer wire	[41,43,59,60,73,146,147,150–152,155,156,159,167,193]
Mackinawite	Subsidiary mineral acting as hydrogenase and electron wire	[42,56,61,160,177–182,184]

#### 4. The Relevance of Accretion Histories to Astrobiology

In the assessments of which worlds might meet the disequilibria requirements for the emergence of life, accretion histories are informative. Within our solar system the terrestrial planets were accreted mainly from iron-nickel meteorites and wet enstatite (MgSiO<sub>3</sub>) chondrites (ECs) [19,163,194,195]. In contrast, the outer planetary zone was populated with CCs comprising phosphoran (P<sub>2</sub>O<sub>5</sub>-bearing) olivine (where P substitutes for Si), serpentine and organic molecules [19,163,194,195]. The CCs represent the all-important contribution of carbon molecules for the emergence of life. However, they formed, along with larger outer solar system bodies, beyond the ‘snow line’ where water and other volatiles condense into ices [196]. While Jupiter’s deep gravitational well had the tendency to block the inward migration of these CCs, sufficient numbers did manage to slip through a gap in the disc as Jupiter got larger and migrated inwards [197]. This resulted in much of the outer asteroid belt also being populated with CCs [197]. Their inward migration may have been responsible for a late heavy bombardment of the inner solar system bodies, adding carbon to the terrestrial planets at the same time [198]. We should note in passing that the migration of Jupiter itself may have had a deleterious effect on Venus’ habitability as it forced the planet into high orbital eccentricities [199]. Such deviations may have driven water loss and brought about a runaway greenhouse notwithstanding the relatively low solar luminosity [199–201].

As we have noted, reduced carbon is ubiquitous in the outer solar system and the Universe at large, making it—in the absence of oxidants—a poor signature for life detection on its own. Even so, another poor life detection signature for terrestrial exoplanets throughout habitable zones in the galaxy are oxygen atmospheres, which may be abiotically-produced from extreme water loss due to high energy UV flux acting to continually disperse hydrogen from vaporizing oceans [202]. Yet, for life to be driven to emerge requires oxidants to provide a positive ‘electrode’ to the reduced molecules hydrothermally focused at a planet or moon’s exterior surface [14]. That is why we contend that the astrobiological signature of interest is the observation of terrestrial water worlds within habitable zones of sufficient mass to drive the physicochemical pressure and stresses such that the bridgmanite-dominant mineralogy of the mantle is poised around the quartz-fayalite-magnetite-(QFM, i.e., SiO<sub>2</sub>-Fe<sup>2+</sup><sub>2</sub>SiO<sub>4</sub>-Fe<sup>2+</sup>Fe<sup>3+</sup><sub>2</sub>O<sub>4</sub>) buffer. This control dictates CO<sub>2</sub> as the stable state of carbon above ~400 °C and thereby a carbon dioxide-rich atmosphere [55].

#### 5. Discussion

Although our planet is largely an amalgam of metal-bearing chondrites, some of them carbonaceous, the volatilsphere (atmosphere and ocean) has been relatively oxidized over the last 4.4 Ga. Carbon occurs as the dioxide rather than hydride, sulfur as sulfide, polysulfide and sulfate, and nitrogen as N<sub>2</sub>, although it was also accompanied in the atmosphere by minor concentrations of nitrogen oxides

that dissolve as nitrate and nitrite in the ocean [28,29,47]. While the latter relatively oxidized gases and ions are results of solar radiation, carbon dioxide has been a major component emanating from our planet since the solar wind blew off the earliest and ephemeral hydrogen atmosphere. This Hadean CO<sub>2</sub> atmosphere was produced, as has been argued, through the oxidation of the lower mantle through disproportionation of ferrous iron in olivine/ringwoodite to produce the ferric-bearing perovskite, bridgmanite, in the lower mantle, while the abandoned native iron tended to exit the lower mantle as it gravitated toward the core, leaving CO<sub>2</sub> as the stable but volatile state of carbon in the mantle. Of course, the Hadean was anything but an equable time in Earth's history and we should expect there to have been major vacillations in the content and temperature of the volatisphere. However, given the 500-million-year duration of the Hadean era, vacillations were more than likely to have intersected the conditions that drove life into being much of this time. We might assume the same held for our sister planet Venus when young, whose atmosphere, without life's draw-down, now boasts ~90 bars of the gas [199].

The question then arises, just how deep does a core-mantle boundary have to be on a wet-rocky world to produce and hold a relatively oxidized atmosphere, i.e., to allow a bridgmanite-dominated lower mantle? The mantle-core boundary depth of Mars today, for example, appears not to reach the threshold of bridgmanite stability, leaving its supposed early atmospheric oxidation state uncertain at best [92,97,203–205]. However, Mars does presently have a CO<sub>2</sub> atmosphere, although with an overall pressure amounting to only 12 mbar [206]. Carbonates too are sparse so whether it once had a higher CO<sub>2</sub> pressure, as supposed by climate modelling, is also debatable [207–209]. More serious is the likelihood that a bridgmanite zone never existed and the Noachian atmosphere would have been H<sub>2</sub> and H<sub>2</sub>O, both being highly soluble in ringwoodite [210–212] (Figure 3).

Nevertheless, all the other rocky, wet, and icy bodies smaller than Mars are very unlikely to have oxidizing atmospheres—i.e., they would be devoid of those electron acceptors required by life—unless they have been and are being, subjected to intense radiation or have entertained large numbers of CO<sub>2</sub>-rich comets.

However, in terms of life's emergence on our planet, we have seen that olivine, and its two "offspring", bridgmanite and serpentine, and accompanying pyrrhotite, did set the stage for life's emergence. Comprising a portion of a membrane separating alkaline hydrothermal fluid from carbonic ocean water, fougérite can act as a hydrogen producer, nitrate/nitrite to ammonium converter, an aminase and phosphate attractor and low entropy environment for its condensation to pyrophosphate (as in olivine and the layered mineral canaphite) [155,156,177,213–215]. At the same time, Ni-bearing iron sulfide, likely mackinawite, and its offspring Ni-bearing greigite, can act as a hydrogenase, hydrogenating catalyst, free energy converter and electron wire or conductor [44,216,217]. Indeed, the contribution by Hudson and collaborators demonstrates the power of a proton gradient (as carbonic acid) across an iron-nickel sulfide, probably mackinawite—an ambient proton motive force—to drive the hydrogenation of CO<sub>2</sub> to the organic molecule, formate (Table 1) (Figure 5). To quote from Hudson et al. [44]; "overall our results suggest that H<sub>2</sub> is the main electron donor, that a large pH gradient is necessary for its oxidation, and that sulfide is insufficient (and might not be required) as an electron donor." Their breakthrough experiment finally answers Leduc's [1] early plea to recognize that "(T)he most important problem of synthetic biology is...the reduction of carbonic acid"!

It may seem that our focus on just these six minerals is overly reductive. For example, haven't clays been at the forefront of mineralization hypotheses and experiments since Bernal [148,192]? But green rust/fougérite is a clay [151] and of the other likely vent precipitates—hisingerite (Fe<sup>3+</sup><sub>2</sub>Si<sub>2</sub>O<sub>5</sub>[OH]<sub>4</sub>·2H<sub>2</sub>O), greenalite (~[Fe<sup>2+</sup>, Fe<sup>3+</sup>]<sub>2</sub>3[Si<sub>2</sub>O<sub>5</sub>][OH]<sub>4</sub>), accompanied by amorphous silica—fougérite is the prime candidate [49,59,146,152]. It has that distinction owing to its variable valence sites, its propensity to juggle electrons and protons in and out of its extensive reactive and flexible internal surfaces, and its proven worth as an abiotic nitrate/nitrite reductase, aminase and generator of hydrogen fuel from water [146,156,158,218,219].

And what of the electron-rich metallic minerals such as awaruite [Ni<sub>3</sub>Fe] that Russell and collaborators [220] had originally called upon to act as a catalyst in the reduction of CO<sub>2</sub> and CO

in the serpentinizing ocean crust? Indeed, in some recent exciting milestone experiments Preiner and collaborators [221] detail how  $H_2$  and  $CO_2$  do react in the presence of awaruite (and magnetite,  $Fe_3O_4$ ) to produce formate, acetate, pyruvate, methanol and methane—all the biochemical products of the acetyl coenzyme A pathway. Moreover, in whole rock two-feed flow reactor serpentinization experiments where the charges included olivine and the reduced iron mineral pyrrhotite White and coworkers [39] recorded formate, acetate and sporadic traces of methane.

On the strength of Preiner and coworkers' one-pot incubation experiments, Martin [222] has argued that awaruite was the “hydrothermal vent alloy” that catalysed the acetyl coenzyme A pathway before the advent of genes—the “Square 1 of bacterial evolution” [222]. But the statement that “serpentinizing systems could have preceded and patterned biotic pathways” does not meet with Endre's [223] stricture that “complexification can only take place in small steps” that produce ever higher efficiencies of entropy production [41,224,225]. As Nick Lane [226] puts it “life transcends chemistry” and is certainly not “a chemical reaction” nor can it be directly compared to a present-day industrial process [222,227].

But the idea that awaruite was a precursor catalyst was mooted at a time when Russell and Hall [4] had considered “the entire hydrothermal system as a pre-living entity and that evolution had brought about a miniaturization of scale from kilometres to millimetres and eventually to micrometres” at the vent [3,128,220,228]. In more recent formulations of the AVT the vent structure itself (where awaruite could not form) has been taken as the site of life's conception; sown and succoured from crustal emanations while bathed in the Hadean ocean [130,229]. Under this view mackinawite and fougérite offer isolated but fixed nickel ions to the prebiotic system in Fe:Ni ratios more consistent with the low solubility of nickel in hydrothermal solutions [7,9,130,182,229–232]. Indeed, the very presence of “residual” awaruite in the oceanic crust is evidence for the low solubility of nickel relative to iron in serpentinizing systems [231,232].

Nevertheless, our focus on the relative concentrations on Earth of the six minerals detailed here should not lull us into a consideration of mere scalar processes. Indeed, a recurring topic in AVT is the vital role of directed active transport; from inward migration of materials in the solar disc, gravitationally-driven convective transport in and on the planet, to ionic, including proton transport or translocation and electron conduction through the membrane—a prelude to vectorial metabolism [233]. And at the alkaline hydrothermal vent itself, one might imagine the fate of the two nickel-bearing iron nanocrystals to be “drawn down” into the entropy-generating vortex of emerging life, dressed in their organic polymers—the precursors of the structure-function-conformational relationships that can still be discerned in life today [145,177,234,235].

## 6. Astrobiological Implications

Studies of the perovskite mineral bridgmanite [(Mg,Fe)SiO<sub>3</sub>], responsible for our oxidized mantle, indicate that ringwoodite suffers a sharp density-increasing phase change to bridgmanite at depth of ~660 km which corresponds to a pressure of 21 GPa. Thus, the original magma ocean and mafic to ultramafic volcanoes would have exhaled carbon mainly as carbon dioxide to the ocean floor, which produced an ocean and atmosphere comprising mostly electron acceptors rather than donors (Figures 1 and 2) [8,55,236,237]. High potential oxidants were also likely available as nitrate and nitrite derived from lightning-driven oxidation of  $N_2$  in the  $CO_2$  atmosphere [28,238]. The reductants consisting of hydrogen and methane, were generated in the lower temperatures of the exothermically-serpentinizing, long reduction-path lengths of the open convective hydrothermal systems feeding the vents and precipitate mounds [55,129,136]. The juxtaposition of the relatively oxidizing and acidulous early Hadean ocean with highly reduced alkaline hydrothermal springs, resulted in the spontaneous precipitates of Ni-bearing, Fe oxyhydroxide and sulfide barriers comprising nanocrysts of fougérite and mackinawite. At times and in places, these barriers induced the necessary redox and pH gradients to force the reduction of  $CO_2$  [42,44], and possibly the oxidation of  $CH_4$ , thus driving the first steps of an autotrophic metabolism [42,130].

However, the wet and rocky bodies in the solar system smaller than Earth and Venus probably have more reduced mantles comprising little or no bridgmanite. This consideration could explain the predominance of methane on the moons of Jupiter and Saturn [48,239–244] and perhaps even early Mars [203–205,245,246]

## 7. Caveats and Limitations

While the several approaches employed here appear to converge on the limiting mineral fundamentals to life's emergence, without which there would be no early CO<sub>2</sub> oxidizing atmospheres and therefore no obvious electrochemical disequilibria required to drive life's emergence, nor to sustain habitability, there are caveats:

(1) AVT assumes that phototrophy cannot emerge *de novo* but evolves via autotrophy and heterotrophy—a point of view open to debate and astrobiological exploration [14];

(2) The assumption derived from climate modelling that Mars once had a CO<sub>2</sub> atmosphere with a pressure exceeding 250 mbar is at odds with the likely high hydrogen fugacity (i.e., the very low oxygen fugacity) of the Martian mantle and the paucity of carbonate outcrop. Although such an early atmosphere has not been disproven, high emissions of H<sub>2</sub> could also explain the warm temperatures at that time [92,203,206,209,247,248];

(3) Some carbon dioxide feedstock on Mars and sub-Mars sized bodies that had no shortage of volatile reductant fuels, might have been provided, and continuously so, from CO<sub>2</sub>-bearing comets in our solar system [88,249];

(4) Oxidants on moons such as Europa may be generated qualitatively by relatively local high energy radiation [250–252];

(5) It is not possible to tell as yet whether the conclusions presented here are applicable to exoplanet exploration. The challenge is to demonstrate the availability of electron acceptors on these other worlds up to 1.6 Earth radii (e.g., [9,253,254]). Indeed, the conclusions reached in this essay would not necessarily apply to M dwarf systems where initial conditions of planetary formation and evolution might have been very different [204,255–260]. For example, 'super-earths' now in the 'habitable zones' of M dwarfs may have suffered irreversible runaway greenhouse conditions (cf. Venus). Later these would have been enveloped with abiotically-produced oxygen atmospheres resulting from a high energy UV flux sufficient to drive water loss from vaporizing oceans through the continual dispersion of H<sub>2</sub> [202]. While such atmospheres are likely to be overwhelmed with oxygen gas and suffer atmospheric warming inimical to life, some smaller examples might have both a hydrosphere as well oxygen pressures suitable for O<sub>2</sub> to act as a positive 'electrode' for life's emergence, a possibility enhanced by the addition of nitric oxides produced by high energy coronal mass injections [29].

**Author Contributions:** M.J.R. developed the theory, and M.J.R. and A.P. researched and wrote the script. All authors have read and agreed to the published version of the manuscript.

**Funding:** This research was funded by NASA, through the NASA Astrobiology Institute under cooperative agreement issued through the Science Mission directorate; No. NNH13ZDA017C (Icy Worlds) at the Jet Propulsion Laboratory. The contributions by AP to this work were carried out at the Jet Propulsion Laboratory, California Institute of Technology, under a contract with the National Aeronautics and Space Administration.

**Acknowledgments:** We thank Isik Kanik, Wolfgang Nitschke, Simon Duval, Elbert Branscomb, Manasvi Lingam, Piero Ugliengo and the late Gianmario Martra for help and discussions. Contributions by AP were carried out at the Jet Propulsion Laboratory, California Institute of Technology, under a contract with the National Aeronautics and Space Administration.

**Conflicts of Interest:** The authors declare no conflict of interest.

## References

1. Leduc, S. A study of molecular physics. *Arch. Roentgen Ray* **1911**, *16*, 202–205. [CrossRef]
2. Longo, G.; Montevil, M.; Sonnenschein, C.; Soto, A.M. In search of principles for a theory of organisms. *J. Biosci.* **2015**, *40*, 955–968. [CrossRef] [PubMed]

3. Russell, M.J.; Daniel, R.M.; Hall, A.J.; Sherringham, J. A hydrothermally precipitated catalytic iron sulphide membrane as a first step toward life. *J. Mol. Evol.* **1994**, *39*, 231–241. [[CrossRef](#)]
4. Russell, M.J.; Hall, A.J. The emergence of life from iron monosulphide bubbles at a submarine hydrothermal redox and pH front. *J. Geol. Soc.* **1997**, *154*, 377–402. [[CrossRef](#)] [[PubMed](#)]
5. Wade, J.; Wood, B.J. Core formation and the oxidation state of the Earth. *Earth Planet. Sci. Lett.* **2005**, *236*, 78–95. [[CrossRef](#)]
6. Russell, M.J. First life. *Am. Sci.* **2006**, *94*, 32–39. [[CrossRef](#)]
7. Elkins-Tanton, L.T. Linked magma ocean solidification and atmospheric growth for Earth and Mars. *Earth Planet. Sci. Lett.* **2008**, *271*, 181–191. [[CrossRef](#)]
8. Hirschmann, M.M. Magma ocean influence on early atmosphere mass and composition. *Earth Planet. Sci. Lett.* **2012**, *341–344*, 48–57. [[CrossRef](#)]
9. Russell, M.J.; Barge, L.M.; Bhartia, R.; Bocanegra, D.; Bracher, P.J.; Branscomb, E.; Kidd, R.; McGlynn, S.; Meier, D.H.; Nitschke, W.; et al. The drive to life on wet and icy worlds. *Astrobiology* **2014**, *14*, 308–343. [[CrossRef](#)]
10. Barge, L.M.; Abedian, Y.; Russell, M.J.; Doloboff, I.J.; Cartwright, J.H.; Kidd, R.D.; Kanik, I. From chemical gardens to fuel cells: Generation of electrical potential and current across self-assembling iron mineral membranes. *Angew. Chem. Int. Ed. Engl.* **2015**, *54*, 8184–8187. [[CrossRef](#)]
11. Waite, J.H., Jr.; Lewis, W.S.; Magee, B.A.; Lunine, J.I.; McKinnon, W.B.; Glein, C.R.; Mousis, O.; Young, D.T.; Brockwell, T.; Westlake, J.; et al. Liquid water on Enceladus from observations of ammonia and <sup>40</sup>Ar in the plume. *Nature* **2009**, *460*, 487–490. [[CrossRef](#)]
12. Yung, Y.L.A.M.; Pinto, J.P. Photochemistry of the atmosphere of Titan: Comparison between model and observations. *Astrophys. J. Suppl. Ser.* **1984**, *55*, 465–506. [[CrossRef](#)] [[PubMed](#)]
13. Hendrix, A.R.; Hurford, T.A.; Barge, L.M.; Bland, M.T.; Bowman, J.S.; Brinckerhoff, W.; Buratti, B.J.; Cable, M.L.; Castillo-Rogez, J.; Collins, G.C.; et al. The NASA roadmap to ocean worlds. *Astrobiology* **2019**, *19*, 1–27. [[CrossRef](#)] [[PubMed](#)]
14. Russell, M.J.; Hall, A.J. The onset and early evolution of life. In *Evolution of Early Earth's Atmosphere, Hydrosphere, and Biosphere—Constraints from Ore Deposits*; Kesler, S.E., Ohmoto, H., Eds.; Geological Society of America Memoir: Boulder, CO, USA, 2006; Volume 198, pp. 1–32.
15. Armstrong, K.; Frost, D.J.; McCammon, C.A.; Rubie, D.C.; Ballaran, B.T. Deep magma ocean formation set the oxidation state of Earth's mantle. *Science* **2019**, *365*, 903–906. [[CrossRef](#)]
16. Deng, J.; Du, Z.; Karki, B.B.; Ghosh, D.B.; Lee, K.K.M. A magma ocean origin to divergent redox evolutions of rocky planetary bodies and early atmospheres. *Nat. Commun.* **2020**, *11*, 2007. [[CrossRef](#)]
17. Tyburczy, J.A.F.B.; Ahrens, T.J. Shock-induced volatile loss from a carbonaceous chondrite: Implications for planetary accretion. *Earth Planet. Sci. Lett.* **1986**, *80*, 201–207. [[CrossRef](#)]
18. Cottrell, A. The natural philosophy of engines. *Contemp. Phys.* **1979**, *20*, 1–10. [[CrossRef](#)]
19. Javoy, M.; Kaminski, E.; Guyot, F.; Andraut, D.; Sanloup, C.; Moreira, M.; Labrosse, S.; Jambon, A.; Agrinier, P.; Davaille, A.; et al. The chemical composition of the Earth: Enstatite chondrite models. *Earth Planet. Sci. Lett.* **2010**, *293*, 259–268. [[CrossRef](#)]
20. Trønnes, R.G.; Baron, M.A.; Eigenmann, K.R.; Guren, M.G.; Heyn, B.H.; Løken, A.; Mohn, C.E. Core formation, mantle differentiation and core-mantle interaction within Earth and the terrestrial planets. *Tectonophysics* **2019**, *760*, 165–198. [[CrossRef](#)]
21. Braukmuller, N.; Wombacher, F.; Funk, C.; Munker, C. Earth's volatile element depletion pattern inherited from a carbonaceous chondrite-like source. *Nat. Geosci.* **2019**, *12*, 564–568. [[CrossRef](#)]
22. Wordsworth, R.D. Atmospheric nitrogen evolution on Earth and Venus. *Earth Planet. Sci. Lett.* **2016**, *447*, 103–111. [[CrossRef](#)]
23. Johnstone, C.P.; Güdel, M.; Stökl, A.; Lammer, H.; Tu, L.; Kislyakova, K.G.; Lüftinger, T.; Odert, P.; Erkaev, N.V.; Dorfi, E.A. The evolution of stellar rotation and the hydrogen atmospheres of habitable-zone terrestrial planets. *Astrophys. J.* **2015**, *815*. [[CrossRef](#)]
24. Ryder, G. Mass flux in the ancient Earth-Moon system and benign implications for the origin of life on Earth. *J. Geophys. Res. Planets* **2002**, *107*, 6-1–6-13. [[CrossRef](#)]
25. Foley, B.J.; Smye, A.J. Carbon cycling and habitability of Earth-sized stagnant lid planets. *Astrobiology* **2018**, *18*, 873–896. [[CrossRef](#)]

26. López-Puertas, M.; Funke, B.; Gil-López, S.; von Clarmann, T.; Stiller, G.P.; Höpfner, M.; Kellmann, S.; Tsidu, M.G.; Fischer, H.; Jackman, C.H. HNO<sub>3</sub>, N<sub>2</sub>O<sub>5</sub>, and ClONO<sub>2</sub> enhancements after the October–November 2003 solar proton events. *J. Geophys. Res. Space Phys.* **2005**, *110*. [[CrossRef](#)]
27. Crutzen, P.J.; Heidt, L.E.; Krasnec, J.P.; Pollock, W.H.; Seiler, W. Biomass burning as a source of atmospheric gases CO, H<sub>2</sub>, N<sub>2</sub>O, NO, CH<sub>3</sub>Cl and COS. *Nature* **1979**, *282*, 253–256. [[CrossRef](#)]
28. Wong, M.L.; Charnay, B.D.; Gao, P.; Yung, Y.L.; Russell, M.J. Nitrogen oxides in early earth's atmosphere as electron acceptors for life's emergence. *Astrobiology* **2017**, *17*, 975–983. [[CrossRef](#)]
29. Lingam, M.; Loeb, A. Colloquium: Physical constraints for the evolution of life on exoplanets. *Rev. Mod. Phys.* **2019**, *91*. [[CrossRef](#)]
30. Gilat, A. Primordial hydrogen-helium degassing, an overlooked major energy source for internal terrestrial processes. *HAIT J. Sci. Eng.* **2005**, *B2*, 125–167.
31. Zgonnik, V. The occurrence and geoscience of natural hydrogen: A comprehensive review. *Earth Sci. Rev.* **2020**, *203*. [[CrossRef](#)]
32. Worman, S.L.; Pratson, L.F.; Karson, J.A.; Schlesinger, W.H. Abiotic hydrogen (H<sub>2</sub>) sources and sinks near the Mid-Ocean Ridge (MOR) with implications for the seafloor biosphere. *Proc. Natl. Acad. Sci. USA* **2020**, *117*, 13283–13293. [[CrossRef](#)] [[PubMed](#)]
33. Mao, H.-k.; Mao, W.L. Key problems of the four-dimensional Earth system. *Matter Radiat. Extrem.* **2020**, *5*. [[CrossRef](#)]
34. Takahashi, E. Speculations on the Archean mantle: Missing link between komatiite and depleted garnet peridotite. *J. Geophys. Res. Solid Earth* **1990**, *95B*, 15941–15954. [[CrossRef](#)]
35. Bédard, J.H. A catalytic delamination-driven model for coupled genesis of Archean crust and sub-continental lithospheric mantle. *Geochim. Cosmochim. Acta* **2006**, *70*, 1188–1214. [[CrossRef](#)]
36. Shock, E.L.; Canovas, P.; Yang, Z.; Boyer, G.; Johnson, K.; Robinson, K.; Fecteau, K.; Windman, T.; Cox, A. Thermodynamics of organic transformations in hydrothermal fluids. *Rev. Mineral. Geochem.* **2013**, *76*, 311–350. [[CrossRef](#)]
37. O'Neill, C.; Debaille, V. The evolution of Hadean–Eoarchean geodynamics. *Earth Planet. Sci. Lett.* **2014**, *406*, 49–58. [[CrossRef](#)]
38. Lang, S.Q.; Fruh-Green, G.L.; Bernasconi, S.M.; Brazelton, W.J.; Schrenk, M.O.; McGonigle, J.M. Deeply-sourced formate fuels sulfate reducers but not methanogens at Lost City hydrothermal field. *Sci. Rep.* **2018**, *8*, 755. [[CrossRef](#)]
39. White, L.M.; Shibuya, T.; Vance, S.D.; Christensen, L.E.; Bhartia, R.; Kidd, R.; Hoffmann, A.; Stucky, G.D.; Kanik, I.; Russell, M.J. Simulating serpentinization as it could apply to the emergence of life using the JPL hydrothermal reactor. *Astrobiology* **2020**, *20*, 307–326. [[CrossRef](#)]
40. Mitchell, P. Vectorial chemistry and the molecular mechanics of chemiosmotic coupling: Power transmission by proticity. *Biochem. Soc. Trans.* **1976**, *4*, 399–430. [[CrossRef](#)]
41. Branscomb, E.; Russell, M.J. Frankenstein or a submarine alkaline vent: Who is responsible for abiogenesis? Part 2: As life is now, so it must have been in the beginning. *Bioessays* **2018**, *40*, e1700182. [[CrossRef](#)]
42. Nitschke, W.; Russell, M.J. Hydrothermal focusing of chemical and chemiosmotic energy, supported by delivery of catalytic Fe, Ni, Mo/W, Co, S and Se, forced life to emerge. *J. Mol. Evol.* **2009**, *69*, 481–496. [[CrossRef](#)] [[PubMed](#)]
43. Russell, M.J. Green rust: The simple organizing 'seed' of all life? *Life* **2018**, *8*, 35. [[CrossRef](#)]
44. Hudson, R.; de Graaf, R.; Strandoo Rodin, M.; Ohno, A.; Lane, N.; McGlynn, S.E.; Yamada, Y.M.A.; Nakamura, R.; Barge, L.M.; Braun, D.; et al. CO<sub>2</sub> reduction driven by a pH gradient. *Proc. Natl. Acad. Sci. USA* **2020**, *117*, 22873–22879. [[CrossRef](#)]
45. Kump, L.R.; Seyfried, W.E. Hydrothermal Fe fluxes during the Precambrian: Effect of low oceanic sulfate concentrations and low hydrostatic pressure on the composition of black smokers. *Earth Planet. Sci. Lett.* **2005**, *235*, 654–662. [[CrossRef](#)]
46. Mielke, R.E.; Russell, M.J.; Wilson, P.R.; McGlynn, S.E.; Coleman, M.; Kidd, R.; Kanik, I. Design, fabrication, and test of a hydrothermal reactor for origin-of-life experiments. *Astrobiology* **2010**, *10*, 799–810. [[CrossRef](#)]
47. Morrison, P.R.; Mojzsis, S.J. Tracing the early emergence of microbial sulfur metabolisms. *Geomicrobiol. J.* **2020**, 1–21. [[CrossRef](#)]
48. Wood, B.J.; Walter, M.J.; Wade, J. Accretion of the Earth and segregation of its core. *Nature* **2006**, *441*, 825–833. [[CrossRef](#)]

49. Meysami, B.; Balaban, M.O.; Teixeira, A.A. Prediction of pH in model systems pressurized with carbon-dioxide. *Biotechnol. Prog.* **1992**, *8*, 149–154. [[CrossRef](#)]
50. Kusakabe, M.; Tanyileke, G.Z.; McCord, S.A.; Schladow, S.G. Recent pH and CO<sub>2</sub> profiles at Lakes Nyos and Monoun, Cameroon: Implications for the degassing strategy and its numerical simulation. *J. Volcanol. Geotherm. Res.* **2000**, *97*, 241–260. [[CrossRef](#)]
51. Cartigny, P.; Pineau, F.; Aubaud, C.; Javoy, M. Towards a consistent mantle carbon flux estimate: Insights from volatile systematics (H<sub>2</sub>O/Ce, δD, CO<sub>2</sub>/Nb) in the North Atlantic mantle (14° N and 34° N). *Earth Planet. Sci. Lett.* **2008**, *265*, 672–685. [[CrossRef](#)]
52. Russell, M.J.; Hall, A.J.; Martin, W. Serpentinization as a source of energy at the origin of life. *Geobiology* **2010**, *8*, 355–371. [[CrossRef](#)] [[PubMed](#)]
53. Cardenas, M.B.; Rodolfo, R.S.; Lapus, M.R.; Cabria, H.B.; Fullon, J.; Gojunco, G.R.; Breecker, D.O.; Cantarero, D.M.; Evaristo, J.; Siringan, F.P.; et al. Submarine groundwater and vent discharge in a volcanic area associated with coastal acidification. *Geophys. Res. Lett.* **2020**, *47*. [[CrossRef](#)]
54. Shock, E.L. Geochemical constraints on the origin of organic compounds in hydrothermal systems. *Origins Life Evol. Biosph.* **1990**, *20*, 331–367. [[CrossRef](#)]
55. Shock, E.L. Chemical environments of submarine hydrothermal systems. *Orig. Life Evol. Biosph.* **1992**, *22*, 67–107. [[CrossRef](#)] [[PubMed](#)]
56. Mielke, R.E.; Robinson, K.J.; White, L.M.; McGlynn, S.E.; McEachern, K.; Bhartia, R.; Kanik, I.; Russell, M.J. Iron-sulfide-bearing chimneys as potential catalytic energy traps at life's emergence. *Astrobiology* **2011**, *11*, 933–950. [[CrossRef](#)] [[PubMed](#)]
57. Tao, C.; Seyfried, W.E., Jr.; Lowell, R.P.; Liu, Y.; Liang, J.; Guo, Z.; Ding, K.; Zhang, H.; Liu, J.; Qiu, L.; et al. Deep high-temperature hydrothermal circulation in a detachment faulting system on the ultra-slow spreading ridge. *Nat. Commun.* **2020**, *11*, 1300. [[CrossRef](#)]
58. German, C.R.; Petersen, S.; Hannington, M.D. Hydrothermal exploration of mid-ocean ridges: Where might the largest sulfide deposits be forming? *Chem. Geol.* **2016**, *420*, 114–126. [[CrossRef](#)]
59. Arrhenius, G.O.; Gedulin, B.; Mojzsis, S. Phosphate in models for chemical evolution. In *Chemical Evolution and Origin of Life*; Ponnampereuma, C., Chela-Flores, J., Eds.; Harpers Brothers: New York, NY, USA, 1993; pp. 23–40.
60. Halevy, I.; Alesker, M.; Schuster, E.M.; Popovitz-Biro, R.; Feldman, Y. A key role for green rust in the Precambrian oceans and the genesis of iron formations. *Nat. Geosci.* **2017**, *10*, 135–139. [[CrossRef](#)]
61. White, L.M.; Bhartia, R.; Stucky, G.D.; Kanik, I.; Russell, M.J. Mackinawite and greigite in ancient alkaline hydrothermal chimneys: Identifying potential key catalysts for emergent life. *Earth Planet. Sci. Lett.* **2015**, *430*, 105–114. [[CrossRef](#)]
62. Russell, M.J.; Nitschke, W.; Branscomb, E. The inevitable journey to being. *Philos. Trans. R Soc. Lond. B Biol. Sci.* **2013**, *368*, 20120254. [[CrossRef](#)]
63. Astumian, R.D. Stochastically pumped adaptation and directional motion of molecular machines. *Proc. Natl. Acad. Sci. USA* **2018**, *115*, 9405–9413. [[CrossRef](#)]
64. Balaz, P.; Achimovicova, M.; Balaz, M.; Billik, P.; Cherkezova-Zheleva, Z.; Criado, J.M.; Delogu, F.; Dutkova, E.; Gaffet, E.; Gotor, F.J.; et al. Hallmarks of mechanochemistry: From nanoparticles to technology. *Chem. Soc. Rev.* **2013**, *42*, 7571–7637. [[CrossRef](#)]
65. Branscomb, E.; Biancalani, T.; Goldenfeld, N.; Russell, M. Escapement mechanisms and the conversion of disequilibria; the engines of creation. *Phys. Rep.* **2017**, *677*, 1–60. [[CrossRef](#)]
66. Carter, C.W., Jr. Escapement mechanisms: Efficient free energy transduction by reciprocally-coupled gating. *Proteins* **2020**, *88*, 710–717. [[CrossRef](#)] [[PubMed](#)]
67. Horowitz, J.M.; Sagawa, T.; Parrondo, J.M. Imitating chemical motors with optimal information motors. *Phys. Rev. Lett.* **2013**, *111*, 010602. [[CrossRef](#)] [[PubMed](#)]
68. Šešelja, D.; Straßer, C. Epistemic justification in the context of pursuit: A coherentist approach. *Synthese* **2014**, *191*, 3111–3141. [[CrossRef](#)]
69. Kaminsky, F.V.; Ryabchikov, I.D.; Wirth, R. A primary natrocarbonatitic association in the Deep Earth. *Mineral. Petrol.* **2015**, *110*, 387–398. [[CrossRef](#)]
70. Majumdar, A.; Wu, M.; Pan, Y.; Iitaka, T.; Tse, J.S. Structural dynamics of basaltic melt at mantle conditions with implications for magma oceans and superplumes. *Nat. Commun.* **2020**, *11*, 4815. [[CrossRef](#)] [[PubMed](#)]

71. Matas, J.; Bass, J.D.; Ricard, Y.; Mattern, E.; Bukowinsky, M.S. On the bulk composition of the lower mantle: Predictions and limitations from generalized inversion of radial seismic profiles. *Geophys. J. Int.* **2007**, *170*, 764–780. [[CrossRef](#)]
72. Proskurowski, G.; Lilley, M.D.; Kelley, D.S.; Olson, E.J. Low temperature volatile production at the Lost City Hydrothermal Field, evidence from a hydrogen stable isotope geothermometer. *Chem. Geol.* **2006**, *229*, 331–343. [[CrossRef](#)]
73. Tosca, N.J.; Jiang, C.Z.; Rasmussen, B.; Muhling, J. Products of the iron cycle on the early Earth. *Free Radic. Biol. Med.* **2019**, *140*, 138–153. [[CrossRef](#)] [[PubMed](#)]
74. Goodrich, C.A. Phosphoran pyroxene and olivine in silicate inclusions in natural iron-carbon alloy, Disko-Island, Greenland. *Geochim. Cosmochim. Acta* **1984**, *48*, 1115–1126. [[CrossRef](#)]
75. Smyth, J.R.; Frost, D.J.; Nestola, F.; Holl, C.M.; Bromiley, G. Olivine hydration in the deep upper mantle: Effects of temperature and silica activity. *Geophys. Res. Lett.* **2006**, *33*, 15. [[CrossRef](#)]
76. Welsch, B.; Hammer, J.; Hellebrand, E. Phosphorus zoning reveals dendritic architecture of olivine. *Geology* **2014**, *42*, 867–870. [[CrossRef](#)]
77. Veter, M.; Foley, S.F.; Mertz-Kraus, R.; Groschopf, N. Trace elements in olivine of ultramafic lamprophyres controlled by phlogopite-rich mineral assemblages in the mantle source. *Lithos* **2017**, *292–293*, 81–95. [[CrossRef](#)]
78. Yamagata, Y.; Watanabe, H.; Saitoh, M.; Namba, T. Volcanic production of pyrophosphate and its relevance to prebiotic evolution. *Nature* **1991**, *352*, 516–519. [[CrossRef](#)]
79. Milman-Barris, M.S.; Beckett, J.R.; Baker, M.B.; Hofmann, A.E.; Morgan, Z.; Crowley, M.R.; Vielzeuf, D.; Stolper, E. Zoning of phosphorus in igneous olivine. *Contrib. Mineral. Petrol.* **2008**, *155*, 739–765. [[CrossRef](#)]
80. De Hoog, J.C.M.; Gall, L.; Cornell, D.H. Trace-element geochemistry of mantle olivine and application to mantle petrogenesis and geothermobarometry. *Chem. Geol.* **2010**, *270*, 196–215. [[CrossRef](#)]
81. Haldorsen, S.; Akan, H.; Çelik, B.; Heun, M. The climate of the Younger Dryas as a boundary for Einkorn domestication. *Veg. Hist. Archaeobotany* **2011**. [[CrossRef](#)]
82. Stow, D. *Vanished Ocean: How Tethys Reshaped the World*; Oxford University Press: Oxford, UK, 2012.
83. Beerling, D.J.; Leake, J.R.; Long, S.P.; Scholes, J.D.; Ton, J.; Nelson, P.N.; Bird, M.; Kantzas, E.; Taylor, L.L.; Sarkar, B.; et al. Farming with crops and rocks to address global climate, food and soil security. *Nat. Plants* **2018**, *4*, 138–147. [[CrossRef](#)]
84. Maruyama, S.; Santosh, M.; Zhao, D. Superplume, supercontinent, and post-perovskite: Mantle dynamics and anti-plate tectonics on the Core–Mantle Boundary. *Gondwana Res.* **2007**, *11*, 7–37. [[CrossRef](#)]
85. Kondo, N.; Yoshino, T.; Matsukage, K.N.; Kogiso, T. Major element composition of an Early Enriched Reservoir: Constraints from <sup>142</sup>Nd/<sup>144</sup>Nd isotope systematics in the early Earth and high-pressure melting experiments of a primitive peridotite. *Prog. Earth Planet. Sci.* **2016**, *3*. [[CrossRef](#)]
86. Bell, D.; Rossman, G.; Maldener, J.; Endisch, D.; Rauch, F. Hydroxide in olivine: A quantitative determination of the absolute amount and calibration of the IR spectrum. *J. Geophys. Res.* **2003**, *108*, 2105. [[CrossRef](#)]
87. Jacobsen, S.D.; Smyth, J.R. Effect of water on the sound velocities of ringwoodite in the transition zone. *Geophys. Monogr. Am. Geophys. Union* **2006**, *168*, 131.
88. Binns, R.A.; Davis, R.J.; Reed, S.J.B. Ringwoodite, natural (Mg,Fe)<sub>2</sub>SiO<sub>4</sub> spinel in the Tenham meteorite. *Nature* **1969**, *221*, 943–944. [[CrossRef](#)]
89. Pearson, D.G.; Brenker, F.E.; Nestola, F.; McNeill, J.; Nasdala, L.; Hutchison, M.T.; Matveev, S.; Mather, K.; Silversmit, G.; Schmitz, S.; et al. Hydrous mantle transition zone indicated by ringwoodite included within diamond. *Nature* **2014**, *507*, 221–224. [[CrossRef](#)] [[PubMed](#)]
90. Genda, H. Origin of Earth's oceans: An assessment of the total amount, history and supply of water. *Geochem. J.* **2016**, *50*, 27–42. [[CrossRef](#)]
91. Mao, Z.; Lin, J.F.; Yang, J.; Inoue, T.; Prakapenka, V.B. Effects of the Fe<sup>3+</sup> spin transition on the equation of state of bridgmanite. *Geophys. Res. Lett.* **2015**, *42*, 4335–4342. [[CrossRef](#)]
92. Wood, B.J. Phase transformations and partitioning relations in peridotite under lower mantle conditions. *Earth Planet. Sci. Lett.* **2000**, *174*, 341–354. [[CrossRef](#)]
93. Liu, X.; Sui, Z.; Fei, H.; Yan, W.; Ma, Y.; Ye, Y. IR Features of hydrous Mg<sub>2</sub>SiO<sub>4</sub>-ringwoodite, unannealed and annealed at 200–600 °C and 1 atm, with implications to hydrogen defects and water-coupled cation disorder. *Minerals* **2020**, *10*, 499. [[CrossRef](#)]
94. Trail, D.; Watson, E.B.; Tailby, N.D. The oxidation state of Hadean magmas and implications for early Earth's atmosphere. *Nature* **2011**, *480*, 79–82. [[CrossRef](#)] [[PubMed](#)]

95. Tschauner, O.; Ma, C.; Beckett, J.R.; Prescher, C.; Prakapenka, V.B.; Rossman, G.R. Mineralogy. Discovery of bridgmanite, the most abundant mineral in Earth, in a shocked meteorite. *Science* **2014**, *346*, 1100–1102. [[CrossRef](#)] [[PubMed](#)]
96. Hansen, V.L. Global tectonic evolution of Venus, from exogenic to endogenic over time, and implications for early Earth processes. *Philos. Trans. R. Soc. A Math. Phys. Eng. Sci.* **2018**, *376*, 26. [[CrossRef](#)] [[PubMed](#)]
97. Wadhwa, M. Redox conditions on small bodies, the Moon and Mars. *Rev. Mineral. Geochem.* **2008**, *68*, 493–510. [[CrossRef](#)]
98. Mahieux, A.; Vandaele, A.C.; Robert, S.; Wilquet, V.; Drummond, R.; Montmessin, F.; Bertaux, J.L. Densities and temperatures in the Venus mesosphere and lower thermosphere retrieved from SOIR on board Venus Express: Carbon dioxide measurements at the Venus terminator. *J. Geophys. Res.* **2012**, *117*, E07001. [[CrossRef](#)]
99. Rivoldini, A.; Van Hoolst, T.; Verhoeven, O.; Mocquet, A.; Dehant, V. Geodesy constraints on the interior structure and composition of Mars. *Icarus* **2011**, *213*, 451–472. [[CrossRef](#)]
100. Fei, Y.; Stagno, V. The redox boundaries of earth's interior. *Elements* **2020**, *16*, 167–172. [[CrossRef](#)]
101. Wetzel, D.T.; Rutherford, M.J.; Jacobsen, S.D.; Hauri, E.H.; Saal, A.E. Degassing of reduced carbon from planetary basalts. *Proc. Natl. Acad. Sci. USA* **2013**, *110*, 8010–8013. [[CrossRef](#)]
102. Stixrude, L.; Lithgow-Bertelloni, C. Geophysics of chemical heterogeneity in the mantle. *Annu. Rev. Earth Planet. Sci.* **2012**, *40*, 569–595. [[CrossRef](#)]
103. Bindi, L.S.; Shim, S.H.; Sharp, T.G.; Xie, X. Evidence for the charge disproportionation of iron in extraterrestrial bridgmanite. *Sci. Adv.* **2020**, *6*, eaay7893. [[CrossRef](#)]
104. Ma, C.; Tschauner, O.; Beckett, J.R.; Liu, Y.; Rossman, G.R.; Sinogeikin, S.V.; Smith, J.S.; Taylor, L.A. Ahrensite,  $\gamma$ -Fe<sub>2</sub>SiO<sub>4</sub>, a new shock-metamorphic mineral from the Tissint meteorite: Implications for the Tissint shock event on Mars. *Geochim. Cosmochim. Acta* **2016**, *184*, 240–256. [[CrossRef](#)]
105. Tiwari, K.; Ghosh, S.; Miyahara, M.; Ray, D. High pressure polymorphs in katol l6 chondrite: Deciphering thermal history and shock conditions. In *Geophysical Research Abstracts*; 2019; p. 18592. Available online: <https://meetingorganizer.copernicus.org/EGU2019/EGU2019-18592-2.pdf> (accessed on 15 November 2020).
106. Goldschmidt, V.M. Geochemical aspects of the origin of complex organic molecules on Earth, as precursors to organic life. *New Biol.* **1952**, *12*, 97–105.
107. Ismailova, L.; Bykova, E.; Bykov, M.; Cerantola, V.; McCammon, C.; Ballaran, T.B.; Bobrov, A.; Sinmyo, R.; Dubrovinskaia, N.; Glazyrin, K.; et al. Stability of Fe, Al-bearing bridgmanite in the lower mantle and synthesis of pure Fe-bridgmanite. *Sci. Adv.* **2016**, *2*, e1600427. [[CrossRef](#)] [[PubMed](#)]
108. Holloway, J.R.; O'Day, P.A. Production of CO<sub>2</sub> and H<sub>2</sub> by dike-eruptive events at mid-ocean ridges: Implications for abiotic organic synthesis and global geochemical cycling. *Int. Geol. Rev.* **2000**, *42*, 673–683. [[CrossRef](#)]
109. Wade, J.; Wood, B.J. The oxidation state and mass of the Moon-forming impactor. *Earth Planet. Sci. Lett.* **2016**, *442*, 186–193. [[CrossRef](#)]
110. Frost, D.J.; Mann, U.; Asahara, Y.; Rubie, D.C. The redox state of the mantle during and just after core formation. *Philos. Trans. R. Soc. A Math. Phys. Eng. Sci.* **2008**, *366*, 4315–4337. [[CrossRef](#)]
111. Frost, D.J.; Liebske, C.; Langenhorst, F.; McCammon, C.A.; Trønnes, R.G.; Rubie, D.C. Experimental evidence for the existence of iron-rich metal in the Earth's lower mantle. *Nature* **2004**, *428*, 409–412. [[CrossRef](#)]
112. Townsend, J.P.; Tsuchiya, J.; Bina, C.R.; Jacobsen, S.D. Water partitioning between bridgmanite and postperovskite in the lowermost mantle. *Earth Planet. Sci. Lett.* **2016**, *454*, 20–27. [[CrossRef](#)]
113. Williams, H.M.; Wood, B.J.; Wade, J.; Frost, D.J.; Tuff, J. Isotopic evidence for internal oxidation of the Earth's mantle during accretion. *Earth Planet. Sci. Lett.* **2012**, *321*, 54–63. [[CrossRef](#)]
114. Herd, C.D.; Borg, L.E.; Jones, J.H.; Papike, J.J. Oxygen fugacity and geochemical variations in the Martian basalts: Implications for Martian basalt petrogenesis and the oxidation state of the upper mantle of Mars. *Geochim. Cosmochim. Acta* **2002**, *66*, 2025–2036. [[CrossRef](#)]
115. Schmidt, M.E.; Schrader, C.M.; McCoy, T.J. The primary fO<sub>2</sub> of basalts examined by the Spirit rover in Gusev Crater, Mars: Evidence for multiple redox states in the martian interior. *Earth Planet. Sci. Lett.* **2013**, *384*, 198–208. [[CrossRef](#)]
116. Shibazaki, Y.; Ohtani, E.; Terasaki, H.; Suzuki, A.; Funakoshi, K. Hydrogen partitioning between iron and ringwoodite: Implications for water transport into the Martian core. *Earth Planet. Sci. Lett.* **2009**, *287*, 463–470. [[CrossRef](#)]
117. Taylor, G.J. The bulk composition of Mars. *Geochemistry* **2013**, *73*, 401–420. [[CrossRef](#)]

118. Yoshizaki, T.; McDonough, W.F. The composition of Mars. *Geochim. Cosmochim. Acta* **2020**, *273*, 137–162. [[CrossRef](#)]
119. Russell, M.J.; Hall, A.J. On the inevitable emergence of life on Mars. In *The Search for Life on Mars*; Hiscox, J.A., Ed.; The British Interplanetary Society: London, UK, 1999; pp. 26–36.
120. Vaughan, D.J.; Craig, J.R. *Mineral. Chemistry of Natural Sulfides*; Cambridge University Press: Cambridge, UK, 1978.
121. Staude, S.; Barnes, S.J.; Markl, G. Interspinifex Ni sulfide ore from Victor South-McLeay, Kambalda, Western Australia. *Miner. Depos.* **2020**. [[CrossRef](#)]
122. Appel, P.W.U. Mineral Occurrences in the 3.6 Ga Old Isua Supracrustal Belt, West Greenland. In *Developments in Precambrian Geology*; Naqvi, S.M., Ed.; Elsevier: Amsterdam, The Netherlands, 1990; Volume 8, pp. 593–603.
123. Hall, A.J. Pyrite pyrrhotite redox reactions in nature. *Mineral. Mag.* **1986**, *50*, 223–229. [[CrossRef](#)]
124. Appel, P.W.U. On the early Archaean Isua iron-formation, West Greenland. *Precamb. Res.* **1980**, *11*, 73–87. [[CrossRef](#)]
125. Macleod, G.; McKeown, C.; Hall, A.J.; Russell, M.J. Hydrothermal and oceanic pH conditions of possible relevance to the origin of life. *Orig. Life Evol. Biosph.* **1994**, *24*, 19–41. [[CrossRef](#)]
126. Lowell, R.P.; Rona, P.A. Seafloor hydrothermal systems driven by the serpentinization of peridotite. *Geophys. Res. Lett.* **2002**, *29*, 1531. [[CrossRef](#)]
127. Escartin, J.; Hirth, G.; Evans, B. Strength of slightly serpentinized peridotites: Implications for the tectonics of oceanic lithosphere. *Geology* **2001**, *29*, 1023–1026. [[CrossRef](#)]
128. Russell, M.J.; Hall, A.J.; Turner, D. In vitro growth of iron sulphide chimneys: Possible culture chambers for origin-of-life experiments. *Terra Nova* **1989**, *1*, 238–241. [[CrossRef](#)]
129. Martin, W.; Baross, J.; Kelley, D.; Russell, M.J. Hydrothermal vents and the origin of life. *Nat. Rev. Microbiol.* **2008**, *6*, 805–814. [[CrossRef](#)] [[PubMed](#)]
130. Nitschke, W.; Russell, M.J. Beating the acetyl coenzyme A-pathway to the origin of life. *Philos. Trans. R Soc. Lond. B Biol. Sci.* **2013**, *368*, 20120258. [[CrossRef](#)] [[PubMed](#)]
131. Tutolo, B.M.; Seyfried, W.E., Jr.; Tosca, N.J. A seawater throttle on H<sub>2</sub> production in Precambrian serpentinizing systems. *Proc. Natl. Acad. Sci. USA* **2020**, *117*, 14756–14763. [[CrossRef](#)] [[PubMed](#)]
132. Williams, Q.; Hemley, R.J. Hydrogen in the deep Earth. *Ann. Rev. Earth Planet. Sci.* **2001**, *29*, 365–418. [[CrossRef](#)]
133. Isaev, E.I.; Skorodumova, N.V.; Ahuja, R.; Vekilov, Y.K.; Johansson, B. Dynamical stability of Fe-H in the Earth's mantle and core regions. *Proc. Natl. Acad. Sci. USA* **2007**, *104*, 9168–9171. [[CrossRef](#)]
134. Bali, E.; Audetat, A.; Keppler, H. Water and hydrogen are immiscible in Earth's mantle. *Nature* **2013**, *495*, 220–222. [[CrossRef](#)]
135. Nédélec, A.; Monnereau, M.; Toplis, M.J. The Hadean-Archaean transition at 4 Ga: From magma trapping in the mantle to volcanic resurfacing of the Earth. *Terra Nova* **2017**, *29*, 218–223. [[CrossRef](#)]
136. Russell, M.J.; Couples, G.D.; Lewis, H.; Pasava, J.; Kribek, B.; Zak, K. SEDEX genesis and super-deep boreholes: Can hydrostatic pressures exist down to the brittle-ductile boundary? In *Mineral. Deposits: From Their Origin to Their Environmental Impact*; Balkema, A.A., Ed.; CRC Press: Boca Raton, FL, USA, 1995; pp. 315–318.
137. McDermott, J.M.; Seewald, J.S.; German, C.R.; Sylva, S.P. Pathways for abiotic organic synthesis at submarine hydrothermal fields. *Proc. Natl. Acad. Sci. USA* **2015**, *112*, 7668–7672. [[CrossRef](#)]
138. Ludwig, K.A.; Shen, C.-C.; Kelley, D.S.; Cheng, H.; Edwards, R.L. U–Th systematics and <sup>230</sup>Th ages of carbonate chimneys at the Lost City Hydrothermal Field. *Geochim. Cosmochim. Acta* **2011**, *75*, 1869–1888. [[CrossRef](#)]
139. Ménez, B. Abiotic hydrogen and methane: Fuels for life. *Elements* **2020**, *16*, 39–46. [[CrossRef](#)]
140. Grozeva, N.G.; Klein, F.; Seewald, J.S.; Sylva, S.P. Chemical and isotopic analyses of hydrocarbon-bearing fluid inclusions in olivine-rich rocks. *Philos. Trans. A Math. Phys. Eng. Sci.* **2020**, *378*, 20180431. [[CrossRef](#)] [[PubMed](#)]
141. Etiope, G.; Lollar, S.B. Abiotic methane on Earth. *Rev. Geophys.* **2013**, *51*, 276–299. [[CrossRef](#)]
142. Russell, M.J.; Nitschke, W. Methane: Fuel or exhaust at the emergence of life? *Astrobiology* **2017**, *17*, 1053–1066. [[CrossRef](#)]
143. Kelley, D.S.; Karson, J.A.; Blackman, D.K.; Früh-Green, G.L.; Butterfield, D.A.; Lilley, M.D.; Olson, E.J.; Schrenk, M.O.; Roe, K.K.; Lebon, G.T.E.A. An off-axis hydrothermal vent field near the Mid-Atlantic Ridge at 30° N. *Nature* **2001**, *412*, 145–149. [[CrossRef](#)]
144. Kelley, D.S.; Karson, J.A.; Früh-Green, G.L.; Yoerger, D.R.; Shank, T.M.; Butterfield, D.A.; Hayes, J.M.; Schrenk, M.O.; Olson, E.J.; Proskurowski, G.; et al. A serpentinite-hosted ecosystem: The lost city hydrothermal field. *Science* **2005**, *307*, 1428–1434. [[CrossRef](#)]

145. Duval, S.K.; Baymann, F.; Schoepp-Cothenet, B.; Branscomb, E.; Russell, M.J.; Nitschke, W. Minerals and the emergence of life. In *Metals in Life Sciences*; Kroneck, P., Torres, S.M.E., Eds.; Walter de Gruyter: Berlin, Germany, 2020.
146. Génin, J.-M.R.; Aïssa, R.; Géhin, A.; Abdelmoula, M.; Benali, O.; Ernsten, V.; Ona-Nguema, G.; Upadhyay, C.; Ruby, C. Fougerite and FeII–III hydroxycarbonate green rust; ordering, deprotonation and/or cation substitution; structure of hydrotalcite-like compounds and mythic ferrosic hydroxide. *Solid State Sci.* **2005**, *7*, 545–572. [[CrossRef](#)]
147. Mackay, A.L. Some aspects of the topochemistry of the iron oxides and hydroxides. In *Reactivity of Solids: Proceedings of the Fourth International Symposium on the Reactivity of Solids, Amsterdam, The Netherlands, 30 May–4 June 1960*; Elsevier: Amsterdam, The Netherlands, 1960; pp. 571–583.
148. Bernal, J.D.; Dasgupta, D.R.; Mackay, A.L. The oxides and hydroxides of iron and their structural inter-relationships. *Clay Miner. Bull.* **1959**, *4*, 15–30. [[CrossRef](#)]
149. Trolard, F.; Bourrié, G. Fougerite a natural layered double hydroxide in gley soil: Habitus, structure, and some properties. In *Clay Minerals in Nature—Their Characterization, Modification and Application*; InTechOpen: London, UK, 2012; pp. 171–188. [[CrossRef](#)]
150. Duval, S.; Baymann, F.; Schoepp-Cothenet, B.; Trolard, F.; Bourrié, G.; Grauby, O.; Branscomb, E.; Russell, M.J.; Nitschke, W. Fougerite: The not so simple progenitor of the first cells. *Interface Focus* **2019**, *9*, 20190063. [[CrossRef](#)]
151. Duval, S.; Branscomb, E.; Trolard, F.; Bourrié, G.; Grauby, O.; Heresanu, V.; Schoepp-Cothenet, B.; Zuchan, K.; Russell, M.J.; Nitschke, W. On the why’s and how’s of clay minerals’ importance in life’s emergence. *Appl. Clay Sci.* **2020**, *195*. [[CrossRef](#)]
152. Arrhenius, G.O. Crystals and life. *Helv. Chim. Acta* **2003**, *86*, 1569–1586. [[CrossRef](#)]
153. Mloszewska, A.M.; Pecoits, E.; Cates, N.L.; Mojzsis, S.J.; O’Neil, J.; Robbins, L.J.; Konhauser, K.O. The composition of Earth’s oldest iron formations: The Nuvvuagittuq Supracrustal Belt (Québec, Canada). *Earth Planet. Sci. Lett.* **2012**, *317–318*, 331–342. [[CrossRef](#)]
154. Mojzsis, S.J.; Harrison, T.M.; Pidgeon, R.T. Oxygen-isotope evidence from ancient zircons for liquid water at the Earth’s surface 4300 Myr ago. *Nature* **2001**, *409*, 178–181. [[CrossRef](#)] [[PubMed](#)]
155. Asimakidou, T.; Makridis, A.; Veintemillas-Verdaguer, S.; Morales, M.P.; Kellartzis, I.; Mitrakas, M.; Vourlias, G.; Angelakeris, M.; Simeonidis, K. Continuous production of magnetic iron oxide nanocrystals by oxidative precipitation. *Chem. Eng. J.* **2020**, *393*. [[CrossRef](#)]
156. Hansen, H.C.B.; Koch, C.B.; Nancke-Krogh, H.; Borggaard, O.K.; Sørensen, J. Abiotic nitrate reduction to ammonium: Key role of green rust. *Environ. Sci. Technol.* **1996**, *30*, 2053–2056. [[CrossRef](#)]
157. Roldan, A.; Hollingsworth, N.; Roffey, A.; Islam, H.U.; Goodall, J.B.; Catlow, C.R.; Darr, J.A.; Bras, W.; Sankar, G.; Holt, K.B.; et al. Bio-inspired CO<sub>2</sub> conversion by iron sulfide catalysts under sustainable conditions. *Chem. Commun.* **2015**, *51*, 7501–7504. [[CrossRef](#)]
158. Barge, L.M.; Flores, E.; Baum, M.M.; VanderVelde, D.G.; Russell, M.J. Redox and pH gradients drive amino acid synthesis in iron oxyhydroxide mineral systems. *Proc. Natl. Acad. Sci. USA* **2019**, *116*, 4828–4833. [[CrossRef](#)]
159. Arrabito, G.; Pezzilli, R.; Prestopino, G.; Medaglia, P.G. Layered double hydroxides in bioinspired nanotechnology. *Crystals* **2020**, *10*, 602. [[CrossRef](#)]
160. Nitschke, W.; McGlynn, S.E.; Milner-White, E.J.; Russell, M.J. On the antiquity of metalloenzymes and their substrates in bioenergetics. *Biochim. Biophys. Acta* **2013**, *1827*, 871–881. [[CrossRef](#)]
161. Muñoz-Santiburcio, D.; Marx, D. Chemistry in nanoconfined water. *Chem. Sci.* **2017**, *8*, 3444–3452. [[CrossRef](#)]
162. Muñoz-Santiburcio, D.; Marx, D. Nanoconfinement in slit pores enhances water self-dissociation. *Phys. Rev. Lett.* **2017**, *119*, 056002. [[CrossRef](#)] [[PubMed](#)]
163. Boesenberg, J.S.; Hewins, R.H. An experimental investigation into the metastable formation of phosphoran olivine and pyroxene. *Geochim. Cosmochim. Acta* **2010**, *74*, 1923–1941. [[CrossRef](#)]
164. Finer, J.T.; Simmons, R.M.; Spudich, J.A. Single myosin molecule mechanics: Piconewton forces and nanometre steps. *Nature* **1994**, *368*, 113–119. [[CrossRef](#)] [[PubMed](#)]
165. Han, H.; Martinez, V.; Forró, C.; Polesel-Maris, J.; Vörös, J.; Zambelli, T. Integration of silver nanowires into SU-8 hollow cantilevers for piezoresistive-based sensing. *Sens. Actuators A Phys.* **2020**, *301*. [[CrossRef](#)]
166. Brockman, J.M.; Su, H.; Blanchard, A.T.; Duan, Y.; Meyer, T.; Quach, M.E.; Glazier, R.; Bazrafshan, A.; Bender, R.L.; Kellner, A.V.; et al. Live-cell super-resolved PAINT imaging of piconewton cellular traction forces. *Nat. Methods* **2020**, *17*, 1018–1024. [[CrossRef](#)]

167. Mullet, M.; Khare, V.; Ruby, C. XPS study of Fe(II)-Fe(III) (oxy)hydroxycarbonate green rust compounds. *Surf. Interface Anal.* **2008**, *40*, 323–328. [[CrossRef](#)]
168. Rimola, A.; Sodupe, M.; Ugliengo, P. Role of mineral surfaces in prebiotic chemical evolution. In silico quantum mechanical studies. *Life* **2019**, *9*, 10. [[CrossRef](#)]
169. Thyveetil, M.A.; Coveney, P.V.; Greenwell, H.C.; Suter, J.L. Computer simulation study of the structural stability and materials properties of DNA-intercalated layered double hydroxides. *J. Am. Chem. Soc.* **2008**, *130*, 4742–4756. [[CrossRef](#)]
170. Wander, M.C.F.; Rosso, K.M.; Schoonen, M.A.A. Structure and charge hopping dynamics in green rust. *J. Phys. Chem. C* **2007**, *111*, 11414–11423. [[CrossRef](#)]
171. Fracchia, M.; Visibile, A.; Ahlberg, E.; Vertova, A.; Minguzzi, A.; Ghigna, P.; Rondinini, S.  $\alpha$ - and  $\gamma$ -FeOOH: Stability, reversibility, and nature of the active phase under hydrogen evolution. *ACS Appl. Energy Mater.* **2018**, *1*, 1716–1725. [[CrossRef](#)]
172. Brown, A.I.; Sivak, D.A. Theory of nonequilibrium free energy transduction by molecular machines. *Chem. Rev.* **2020**, *120*, 434–459. [[CrossRef](#)] [[PubMed](#)]
173. Mitchell, P. The origin of life and the formation and organizing functions of natural membranes. In *The Origin of Life on the Earth*; Oparin, A.I., Braunshtein, A.E., Pasynskiĭ, A.G., Pavlovskaya, T.E., Eds.; Pergamon Press: New York, NY, USA, 1959; pp. 437–443. [[CrossRef](#)]
174. Hoffmann, P.M. *Life's Ratchet: How Molecular Machines Extract Order from Chaos*; Basic Books: New York, NY, USA, 2012.
175. Heidary, N.; Kornienko, N.; Kalathil, S.; Fang, X.; Ly, K.H.; Greer, H.F.; Reisner, E. Disparity of cytochrome utilization in anodic and cathodic extracellular electron transfer pathways of geobacter sulfurreducens biofilms. *J. Am. Chem. Soc.* **2020**, *142*, 5194–5203. [[CrossRef](#)] [[PubMed](#)]
176. Horowitz, N.E.; Shevchenko, E.V.; Park, J.; Lee, E.; Xie, J.; Chen, B.; Zhong, Y.; Filatov, A.S.; Anderson, J.S. Synthesis, modular composition, and electrochemical properties of lamellar iron sulfides. *J. Mater. Chem. A* **2020**, *8*, 15834–15844. [[CrossRef](#)]
177. Barge, L.M.; Jones, J.-P.; Pagano, J.J.; Martinez, E.; Bescup, J. Three-dimensional analysis of a simulated prebiotic hydrothermal chimney. *ACS Earth Space Chem.* **2020**, *4*, 1663–1669. [[CrossRef](#)]
178. Bourdoiseau, J.A.; Jeannin, M.; Sabot, R.; Rémazeilles, C.; Refait, P. Characterisation of mackinawite by Raman spectroscopy: Effects of crystallisation, drying and oxidation. *Corros. Sci.* **2008**, *50*, 3247–3255. [[CrossRef](#)]
179. Rickard, D.; Griffith, A.; Oldroyd, A.; Butler, I.B.; Lopez-Capel, E.; Manning, D.A.C.; Apperley, D.C. The composition of nanoparticulate mackinawite, tetragonal iron(II) monosulfide. *Chem. Geol.* **2006**, *235*, 286–298. [[CrossRef](#)]
180. Sano, Y.; Kyono, A.; Yoneda, Y.; Isaka, N.; Takagi, S.; Yamamoto, G.I. Structure changes of nanocrystalline mackinawite under hydrothermal conditions. *J. Mineral. Petrol. Sci.* **2020**, *115*, 261–275. [[CrossRef](#)]
181. Arakaki, T.; Morse, J.W. Coprecipitation and adsorption of Mn (II) with mackinawite (FeS) under conditions similar to those found in anoxic sediments. *Geochim. Cosmochim. Acta* **1993**, *57*, 9–14. [[CrossRef](#)]
182. Morse, J.W.; Arakaki, T. Adsorption and coprecipitation of divalent metals with mackinawite (FeS). *Geochim. Cosmochim. Acta* **1993**, *57*, 3635–3640. [[CrossRef](#)]
183. Volbeda, A.; Fontecilla-Camps, J.C. Catalytic nickel–iron–sulfur clusters: From minerals to enzymes. In *Bioorganometallic Chemistry*; Berlin, H., Ed.; Springer: Berlin/Heidelberg, Germany, 2006; pp. 57–82.
184. Wilkin, R.T.; Beak, D.G. Uptake of nickel by synthetic mackinawite. *Chem. Geol.* **2017**, *462*, 15–29. [[CrossRef](#)]
185. Sojo, V.; Herschy, B.; Whicher, A.; Camprubi, E.; Lane, N. The origin of life in alkaline hydrothermal vents. *Astrobiology* **2016**, *16*, 181–197. [[CrossRef](#)] [[PubMed](#)]
186. Vasiliadou, R.; Dimov, N.; Szita, N.; Jordan, S.F.; Lane, N. Possible mechanisms of CO<sub>2</sub> reduction by H<sub>2</sub> via prebiotic vectorial electrochemistry. *Interface Focus* **2019**, *9*, 20190073. [[CrossRef](#)] [[PubMed](#)]
187. Cao, F.; Hu, W.; Zhou, L.; Shi, W.; Song, S.; Lei, Y.; Wang, S.; Zhang, H. 3D Fe<sub>3</sub>S<sub>4</sub> flower-like microspheres: High-yield synthesis via a biomolecule-assisted solution approach, their electrical, magnetic and electrochemical hydrogen storage properties. *Dalton. Trans.* **2009**, 9246–9252. [[CrossRef](#)] [[PubMed](#)]
188. Kadirvel, P.; Subramanian, A.; Sridharan, N.; Subramanian, S.; Vimaladhasan, S.; Anishetty, S. Molecular dynamics simulation study of Plasmodium falciparum and Escherichia coli SufA: Exploration of conformational changes possibly involved in iron-sulfur cluster transfer. *J. Biomolec. Struct. Dyn.* **2020**. [[CrossRef](#)]
189. Santos-Carballal, D.; Roldan, A.; De Leeuw, N.H. CO<sub>2</sub> reduction to acetic acid on the greigite Fe<sub>3</sub>S<sub>4</sub>{111} surface. *Faraday Discuss.* **2020**. [[CrossRef](#)]

190. Branscomb, E.; Russell, M.J. Turnstiles and bifurcators: The disequilibrium converting engines that put metabolism on the road. *Biochim. Biophys. Acta-Bioenerg.* **2013**, *1827*, 62–78. [[CrossRef](#)]
191. Pinske, C.; Sargent, F. Exploring the directionality of Escherichia coli formate hydrogenlyase: A membrane-bound enzyme capable of fixing carbon dioxide to organic acid. *Microbiologyopen* **2016**, *5*, 721–737. [[CrossRef](#)]
192. Cairns-Smith, A.G.; Hall, A.J.; Russell, M.J. Chapter 9 Mineral theories of the origin of life and an iron sulfide example. *Orig. life Evol. Biosph.* **1992**, *22*, 161–180. [[CrossRef](#)]
193. Branscomb, E.; Russell, M.J. Why the Submarine Alkaline Vent is the Most Reasonable Explanation for the Emergence of Life. *Bioessays* **2019**, *41*. [[CrossRef](#)]
194. Piani, L.; Marrocchi, Y.; Rigaudier, T.; Vacher, L.G.; Thomassin, D.; Marty, B. Earth's water may have been inherited from material similar to enstatite chondrite meteorites. *Science* **2020**, *369*, 1110–1113. [[CrossRef](#)]
195. Jacquet, E.; Pignatale, F.C.; Chaussidon, M.; Charnoz, S. Fingerprints of the protosolar cloud collapse in the Solar System. II. Nucleosynthetic anomalies in meteorites. *Astrophys. J.* **2019**, *884*, 32. [[CrossRef](#)]
196. Raymond, S.N.; Quinn, T.; Lunine, J.I. High-resolution simulations of the final assembly of Earth-like planets 2: Water delivery and planetary habitability. *Astrobiology* **2007**, *7*, 66–84. [[CrossRef](#)] [[PubMed](#)]
197. Kruijjer, T.S.; Kleine, T.; Borg, L.E. The great isotopic dichotomy of the early Solar System. *Nat. Astron.* **2019**, *4*, 32–40. [[CrossRef](#)]
198. Nesvorný, D. Dynamical evolution of the early Solar System. *Ann. Rev. Astron. Astrophys.* **2018**, *56*, 137–174. [[CrossRef](#)]
199. Kane, S.R.; Vervoort, P.; Horner, J.; Pozuelos, F.J. Could the migration of Jupiter have accelerated the atmospheric evolution of venus? *Planet. Sci. J.* **2020**, *1*. [[CrossRef](#)]
200. Bahcall, J.N.; Pinsonneault, M.H.; Basu, S. Solar models: Current epoch and time dependences, neutrinos, and helioseismological properties. *Astrophys. J.* **2001**, *555*, 990–1012. [[CrossRef](#)]
201. Palubski, I.Z.; Shields, A.L.; Deitrick, R. Habitability and Water Loss Limits on Eccentric Planets Orbiting Main-sequence Stars. *arXiv* **2020**, arXiv:2001.02228. [[CrossRef](#)]
202. Luger, R.; Barnes, R. Extreme water loss and abiotic O<sub>2</sub> buildup on planets throughout the habitable zones of M dwarfs. *Astrobiology* **2015**, *15*, 119–143. [[CrossRef](#)]
203. Edwards, C.S.; Ehlmann, B.L. Carbon sequestration on Mars. *Geology* **2015**, *43*, 863–866. [[CrossRef](#)]
204. Hu, R.; Kass, D.M.; Ehlmann, B.L.; Yung, Y.L. Tracing the fate of carbon and the atmospheric evolution of Mars. *Nat. Commun.* **2015**, *6*, 10003. [[CrossRef](#)]
205. Wong, M.L.; Friedson, A.J.; Willacy, K.; Shia, R.L.; Yung, Y.L.; Russell, M.J. A methane-rich early Mars: Implications for habitability and the emergence of life. In Proceedings of the Habitable Worlds 2017: A System Science Workshop, Laramie, Wyoming, 13–17 November 2017. LPI Contrib. No. 1965.
206. Putzig, N.E.; Smith, I.B.; Perry, M.R.; Foss, F.J., 2nd; Campbell, B.A.; Phillips, R.J.; Seu, R. Three-dimensional radar imaging of structures and craters in the Martian polar caps. *Icarus* **2018**, *308*, 138–147. [[CrossRef](#)] [[PubMed](#)]
207. Bultel, B.; Viennet, J.C.; Poulet, F.; Carter, J.; Werner, S.C. Detection of carbonates in martian weathering profiles. *J. Geophys. Res. Planets* **2019**, *124*, 989–1007. [[CrossRef](#)]
208. Heard, A.W.; Kite, E.S. A probabilistic case for a large missing carbon sink on Mars after 3.5 billion years ago. *Earth Planet. Sci. Lett.* **2020**, *531*. [[CrossRef](#)]
209. Urata, R.A.; Toon, O.B. Simulations of the martian hydrologic cycle with a general circulation model: Implications for the ancient martian climate. *Icarus* **2013**, *226*, 229–250. [[CrossRef](#)]
210. Khan, A.; Liebske, C.; Rozel, A.; Rivoldini, A.; Nimmo, F.; Connolly, J.A.D.; Plesa, A.C.; Giardini, D. A geophysical perspective on the bulk composition of mars. *J. Geophys. Res. Planets* **2018**, *123*, 575–611. [[CrossRef](#)]
211. O'Rourke, J.G.; Shim, S.H. Hydrogenation of the martian core by hydrated mantle minerals with implications for the early dynamo. *J. Geophys. Res. Planets* **2019**, *124*, 3422–3441. [[CrossRef](#)]
212. Plesa, A.C.; Padovan, S.; Tosi, N.; Breuer, D.; Grott, M.; Wiczczonek, M.A.; Spohn, T.; Smrekar, S.E.; Banerdt, W.B. The thermal state and interior structure of Mars. *Geophys. Res. Lett.* **2018**, *45*, 12198–112209. [[CrossRef](#)]
213. Hooks, M.R.; Webster, P.; Weber, J.M.; Perl, S.; Barge, L.M. Effects of amino acids on iron-silicate chemical garden precipitation. *Langmuir* **2020**, *36*, 5793–5801. [[CrossRef](#)]
214. Mayen, L.; Jensen, N.D.; Desbord, M.; Laurencin, D.; Gervais, C.; Bonhomme, C.; Smith, M.E.; Porcher, F.; Elkaim, E.; Charvillat, C.; et al. Advances in the synthesis and structure of  $\alpha$ -canaphite: A multitool and multiscale study. *CrystEngComm* **2020**, *22*, 3130–3143. [[CrossRef](#)]
215. Wang, Q.; Barge, L.M.; Steinbock, O. Microfluidic production of pyrophosphate catalyzed by mineral membranes with steep pH gradients. *Chemistry* **2019**, *25*, 4732–4739. [[CrossRef](#)]

216. Zeng, S.-L.; Wang, H.-X.; Dong, C. Synthesis and electrical conductivity of nanocrystalline tetragonal FeS. *Chin. Phys. B* **2014**, *23*. [[CrossRef](#)]
217. Li, Y.; Kitadai, N.; Nakamura, R. Chemical diversity of metal sulfide minerals and its implications for the origin of life. *Life* **2018**, *8*, 46. [[CrossRef](#)] [[PubMed](#)]
218. Russell, M.J. Life is a verb, not a noun. *Geology* **2017**, *45*, 1143–1144. [[CrossRef](#)]
219. Barge, L.M.; Flores, E.; VanderVelde, D.G.; Weber, J.M.; Baum, M.M.; Castonguay, A. Effects of Geochemical and Environmental Parameters on Abiotic Organic Chemistry Driven by Iron Hydroxide Minerals. *J. Geophys. Res. Planets* **2020**, *125*. [[CrossRef](#)]
220. Russell, M.J.; Daia, D.E.; Hall, A.J. The emergence of life from FeS bubbles at alkaline hot springs in an acid ocean. In *Thermophiles: The Keys to Molecular Evolution and the Origin of Life?* Adams, M.W.W., Ljungdahl, L.G., Wiegel, J., Eds.; Taylor and Francis: London, UK; Washington, DC, USA, 1998; pp. 77–126.
221. Preiner, M.; Igarashi, K.; Muchowska, K.B.; Yu, M.; Varma, S.J.; Kleinermaans, K.; Nobu, M.K.; Kamagata, Y.; Tuysuz, H.; Moran, J.; et al. A hydrogen-dependent geochemical analogue of primordial carbon and energy metabolism. *Nat. Ecol. Evol.* **2020**, *4*, 534–542. [[CrossRef](#)]
222. Martin, W.F. Older than genes: The acetyl CoA pathway and origins. *Front. Microbiol.* **2020**, *11*, 817. [[CrossRef](#)]
223. Endres, R.G. Entropy production selects nonequilibrium states in multistable systems. *Sci. Rep.* **2017**, *7*, 14437. [[CrossRef](#)]
224. Cartwright, J.H.E.; Russell, M.J. The origin of life: The submarine alkaline vent theory at 30. *Interface Focus* **2019**, *9*. [[CrossRef](#)]
225. Cook, J.; Endres, R.G. Thermodynamics of switching in multistable non-equilibrium systems. *J. Chem. Phys.* **2020**, *152*. [[CrossRef](#)]
226. Lane, N. Why are cells powered by proton gradients? *Nat. Educ.* **2010**, *3*, 18.
227. Preiner, M.; Xavier, J.C.; Sousa, F.L.; Zimorski, V.; Neubeck, A.; Lang, S.Q.; Greenwell, H.C.; Kleinermaans, K.; Tuysuz, H.; McCollom, T.M.; et al. Serpentinization: Connecting geochemistry, ancient metabolism and industrial hydrogenation. *Life* **2018**, *8*, 41. [[CrossRef](#)] [[PubMed](#)]
228. Neal, C.; Stanger, G. Hydrogen generation from mantle source rocks in Oman. *Earth Planet. Sci. Lett.* **1983**, *66*, 315–320. [[CrossRef](#)]
229. Russell, M.J.; Hall, A.J. From geochemistry to biochemistry: Chemiosmotic coupling and transition element clusters in the onset of life and photosynthesis. *Geochem. News* **2002**, *113*, 6–12.
230. Refait, P.; Drissi, H.; Marie, Y.; Genin, J.M.R. The substitution of Fe<sup>2+</sup> ions by Ni<sup>2+</sup> ions in green rust one compounds. *Hyperfine Interact.* **1994**, *90*, 389–394. [[CrossRef](#)]
231. Shock, E.L.; Sassani, D.C.; Willis, M.; Sverjensky, D.A. Inorganic species in geologic fluids: Correlations among standard molal thermodynamic properties of aqueous ions and hydroxide complexes. *Geochim. Cosmochim. Acta* **1997**, *61*, 907–950. [[CrossRef](#)]
232. Lin, S.; Popp, R.K. Solubility and complexing of Ni in the system NiO-H<sub>2</sub>O-HCl. *Geochim. Cosmochim. Acta* **1984**, *48*, 2713–2722. [[CrossRef](#)]
233. Mitchell, P. Metabolism, transport, and morphogenesis: Which drives which? *J. Gen. Microbiol.* **1962**, *29*, 25–37. [[CrossRef](#)]
234. Milner-White, E.J. Protein three-dimensional structures at the origin of life. *Interface Focus* **2019**, *9*, 20190057. [[CrossRef](#)]
235. Szilagy, R.K.; Hanscam, R.; Shepard, E.M.; McGlynn, S.E. Natural selection based on coordination chemistry: Computational assessment of [4Fe-4S]-maquettes with non-coded amino acids. *Interface Focus* **2019**, *9*, 20190071. [[CrossRef](#)]
236. Dasgupta, R.; Hirschmann, M.M. Melting in the Earth's deep upper mantle caused by carbon dioxide. *Nature* **2006**, *440*, 659–662. [[CrossRef](#)]
237. Yung, Y.L.; McElroy, M.B. Fixation of nitrogen in the prebiotic atmosphere. *Science* **1979**, *203*, 1002–1004. [[CrossRef](#)] [[PubMed](#)]
238. Ducluzeau, A.-L.; van Lis, R.; Duval, S.; Schoepp-Cothenet, B.; Russell, M.J.; Nitschke, W. Was nitric oxide the first deep electron sink? *Trends Biochem. Sci.* **2009**, *34*, 9–15. [[CrossRef](#)] [[PubMed](#)]
239. Bouquet, A.; Mousis, O.; Waite, J.H.; Picaud, S. Possible evidence for a methane source in Enceladus' ocean. *Geophys. Res. Lett.* **2015**, *42*, 1334–1339. [[CrossRef](#)]
240. Dorofeeva, V.A. Genesis of volatile components at Saturn's regular satellites. Origin of Titan's atmosphere. *Geochem. Intern.* **2016**, *54*, 7–26. [[CrossRef](#)]

241. Girard, J.A.; Amulele, G.; Farla, R.; Mohiuddin, A.; Karato, S.I. Shear deformation of bridgmanite and magnesiowüstite aggregates at lower mantle conditions. *Science* **2016**, *351*, 144–147. [[CrossRef](#)] [[PubMed](#)]
242. Gu, T.; Li, M.; McCammon, C.; Lee, K.K.M. Redox-induced lower mantle density contrast and effect on mantle structure and primitive oxygen. *Nat. Geosci.* **2016**, *9*, 723–727. [[CrossRef](#)]
243. Righter, K.; Herd, C.D.K.; Boujibar, A. Redox Processes in early earth accretion and in terrestrial bodies. *Elements* **2020**, *16*, 161–166. [[CrossRef](#)]
244. Zolotov, M.; Kargel, J. On the chemical composition of europa's icy shell, ocean, and underlying rocks. *Geology* **2009**. [[CrossRef](#)]
245. Wadhwa, M. Redox state of Mars' upper mantle and crust from Eu anomalies in shergottite pyroxenes. *Science* **2001**, *291*, 1527–1530. [[CrossRef](#)]
246. Herd, C.D. The oxygen fugacity of olivine-phyric Martian basalts and the components within the mantle and crust of Mars. *Meteor. Planet. Sci.* **2003**, *38*, 1793–1805. [[CrossRef](#)]
247. Wordsworth, R.; Kalugina, Y.; Lokshtanov, S.; Vigasin, A.; Ehlmann, B.; Head, J.; Sanders, C.; Wang, H. Transient reducing greenhouse warming on early Mars. *Geophys. Res. Lett.* **2017**, *44*, 665–671. [[CrossRef](#)]
248. Deng, Z.; Moynier, F.; Villeneuve, J.; Jensen, N.K.; Liu, D.; Cartigny, P.; Mikouchi, T.; Siebert, J.; Agranier, A.; Chaussidon, M.; et al. Early oxidation of the martian crust triggered by impacts. *Sci. Adv.* **2020**, *6*, eabc4941. [[CrossRef](#)] [[PubMed](#)]
249. Ootsubo, T.; Kawakita, H.; Hamada, S.; Kobayashi, H.; Yamaguchi, M.; Usui, F.; Nakagawa, T.; Ueno, M.; Ishiguro, M.; Sekiguchi, T.; et al. Akari near-Infrared Spectroscopic Survey for CO<sub>2</sub> in 18 Comets. *Astrophys. J.* **2012**, *752*. [[CrossRef](#)]
250. Hand, K.P.; Sotin, C.; Hayes, A.; Coustenis, A. On the habitability and future exploration of ocean worlds. *Space Sci. Rev.* **2020**, *216*. [[CrossRef](#)]
251. Russell, M.J.; Murray, A.E.; Hand, K.P. The possible emergence of life and differentiation of a shallow biosphere on irradiated icy worlds: The example of Europa. *Astrobiology* **2017**, *17*, 1265–1273. [[CrossRef](#)]
252. Vance, S.D.; Hand, K.P.; Pappalardo, R.T. Geophysical controls of chemical disequilibria in Europa. *Geophys. Res. Lett.* **2016**, *43*, 4871–4879. [[CrossRef](#)]
253. Nealson, K.H. The limits of life on Earth and searching for life on Mars. *J. Geophys. Res. Planets* **1997**, *102*, 23675–23686. [[CrossRef](#)]
254. Rogers, L.A. Most 1.6 earth-radius planets are not rocky. *Astrophys. J.* **2015**, *801*. [[CrossRef](#)]
255. Cowan, N.B.; Abbot, D.S. Water cycling between ocean and mantle: Super-earths need not be waterworlds. *Astrophys. J.* **2014**, *781*. [[CrossRef](#)]
256. Narita, N.; Enomoto, T.; Masaoka, S.; Kusakabe, N. Titania may produce abiotic oxygen atmospheres on habitable exoplanets. *Sci. Rep.* **2015**, *5*, 13977. [[CrossRef](#)]
257. Noack, L.; Höning, D.; Rivoldini, A.; Heistracher, C.; Zimov, N.; Journaux, B.; Lammer, H.; Van Hoolst, T.; Bredehöft, J.H. Water-rich planets: How habitable is a water layer deeper than on Earth? *Icarus* **2016**, *277*, 215–236. [[CrossRef](#)]
258. Meadows, V.S. Reflections on O<sub>2</sub> as a biosignature in exoplanetary atmospheres. *Astrobiology* **2017**, *17*, 1022–1052. [[CrossRef](#)]
259. Ponce, A. Radionuclide-induced defect sites in iron-bearing minerals may have accelerated the emergence of life. *Interface Focus* **2019**, *9*, 20190085. [[CrossRef](#)] [[PubMed](#)]
260. Olson, S.L.; Jansen, M.; Abbot, D.S. Oceanographic considerations for exoplanet life detection. *Astrophys. J.* **2020**, *895*. [[CrossRef](#)]

**Publisher's Note:** MDPI stays neutral with regard to jurisdictional claims in published maps and institutional affiliations.



© 2020 by the authors. Licensee MDPI, Basel, Switzerland. This article is an open access article distributed under the terms and conditions of the Creative Commons Attribution (CC BY) license (<http://creativecommons.org/licenses/by/4.0/>).